

GRAVITY ANOMALIES OF THE EASTERN MEDITERRANEAN*

H. Fethullah ÖZELÇİ

Mineral Research and Exploration Institute of Turkey

ABSTRACT. — Eastern Mediterranean gravity anomalies, supplemented by Anatolian anomalies and linear correlation coefficient analysis of gravity values and topographic elevation along several profiles in Anatolia are evaluated.

It is observed that the hundred milligals difference in gravity values, the gravity anomaly-topography relations and peculiar isostatic conditions seen in Eastern Mediterranean are also seen over Anatolia.

It is observed that, while The Eastern Mediterranean is over-compensated with respect to gravity anomalies, Anatolia is undercompensated.

In the light of peculiar isostatic conditions and gravity value-topographic relations, it is suggested that the compensation conditions in the region are due to a low-velocity asthenosphere in the mantle.

Local positive isostatic anomalies of Cyprus and Aegean sea are explained by local, near surface heavy material over the low-velocity asthenosphere.

INTRODUCTION

The Eastern Mediterranean Region, lying in the seismic zone extending from Gibraltar in the west to the Indonesian Island Arcs in the east, with its island-arc-type structures, has been an interesting area of gravitational study since 1930. With the recent developments, these studies gained further importance.

Vening Meinesz (1932), Cassinis and De Pica (1935), Mace (1939), Cassinis (1941), Cooper *et al.* (1952), Harrison (1955), Girdler and Harrison (1957), Fahlquist (1963), Gass and Masson-Smith (1963) published the early results of the gravity surveys in the region, helping to reach some important results on the gravitational conditions in the area.

Mace (1939) determined Hayford isostatic anomaly over Cyprus and observed that it was highly positive and reached 173 milligals.

Harrison (1955), observing the 750 meters elevated location of Upper Pliocene sediments, the raised beaches along the coast and the rejuvenated rivers in the Troodos Massif in Cyprus, determined that Cyprus is actually rising. Using submarine gravity measurements in the region carried out by Cooper *et al.* (1952), he also observed that the region was highly faulted and the Bouguer anomaly and the depth of the sea bed had inverse relation in the Crete region. He explained his last observation as the crust being raised with the mantle.

Fahlquist (1963) observed that the Eastern Mediterranean gravity anomalies were 100 milligals lower than the Western Mediterranean and other oceans.

Gass and Masson-Smith (1963) explained the Cyprus gravity anomaly by a heavy mantle material raised to the surface at Troodos massif and observed the local character of this anomaly. Later, Gass (1968) explained the same anomaly, under the concept of plate tectonics, with the overthrust ocean floor over the African plate; thus explaining the mechanism that brought the heavier mantle material to the surface.

Rabinowitz and Ryan (1970), using the gravity profiles taken on the Robert D. Conrad ship by the Lamont Doherty Geological Observatory in 1965 and connecting these profiles with the previous gravity data in the area, for the first time were able to publish their evaluations of the general gravity anomalies of the region on regional scale. Utilizing shallow reflection results and heat flow conditions together with gravity data, they evaluated the general structural conditions in the Eastern Mediterranean Basin and they related gravity anomalies to the variation of surface sedimentary cover thicknesses. Observing a narrow and continuous gravity low to the south of Cretan Arc they suggested that Crete is actually an Island Arc.

Woodside and Bowin (1970), using all the gravity data available in the region, together with that obtained on the Chain ship in 1966 by Woods Hole Oceanographic Institution, studied the crustal structure of the Eastern Mediterranean Basin. In their more detailed work, it is observed that the gravity low to the south of the Cretan Arc is not a narrow continuous zone but an alternation of local gravity lows and highs. In their studies, the gravity anomalies are related to the variation of the thickness of the crust in the region. Having no deep refraction profiles in the area, they determined crustal thickness using standard crustal column at a point where free-air anomaly is zero, and by theoretically fitting observed gravity anomalies with those calculated from assumed crustal configuration. Thus they inferred the crustal thickness variations in the Eastern Mediterranean Basin from gravity data. Their calculations indicated that the crust thickens towards the north. By comparing free-air and Bouguer anomalies, they determined that the gravity anomalies should arise from the depth variations of the mantle.

Gravity surveys in the Eastern Mediterranean Basin are still being carried out and new gravity data is continuously being added to that already available. Hoping that the gravity data in Anatolia would help in understanding the general tectonics and the cause of the gravity anomalies of the Eastern Mediterranean Region, in this thesis Woodside and Bowin's gravity data have been connected to that obtained in Anatolia, and a more general evaluation of the strange gravitational conditions in the region is made. It is suggested that the gravity anomalies of the Eastern Mediterranean Region are very closely connected to the conditions in the mantle.

THE GENERAL CHARACTERISTICS OF THE GRAVITY ANOMALIES

In Figure 1 the Eastern Mediterranean Region Bouguer Anomaly Map is shown. The gravity anomalies of the Eastern Mediterranean Basin are from Woodside and Bowin (1970); the Anatolian anomalies were obtained from widely-spaced observations at gravity base stations in the airports and detailed gravity profiles run across Taurus Mountain Range and along the Aegean coast. In the anomaly calculations 2.67 gm/cm^3 density was used. Anomalies in Tuz Gölü and Konya region were obtained by connecting detailed gravity work that was available. To eliminate any spurious anomalies that may have arisen through errors in the connection of several gravity survey results and to eliminate local effects the contour interval has been chosen as 20 milligals. For this contour interval, ± 4 milligal accuracy of the gravity data was considered acceptable.

In terms of their general characteristics, the gravity anomalies of the region may be described as follows:

1. As it would be expected under normal isostatic conditions, the gravity anomalies in the region, with the exception of Cyprus, the Aegean Islands and narrow coastal regions, are negative over land areas and positive over water-covered areas. In general the zero Bouguer anomaly contour roughly follows the coast line.

2. Hundred-milligal anomalies of variable size "prevail in the Basin region.

3. In the southern part of the Mediterranean Basin, a broad anomaly, covering a large part of this section, runs along a roughly E-W direction and is interrupted suddenly in the east (Anomaly no. 3 on the map).

4. In the North, over Anatolia, a roughly E-W-trending broad anomaly starts where the anomaly in item 3 ends and extends eastward to cover the whole of Eastern Anatolia (Anomaly no. 4).

5. The Cyprus Anomaly (Anomaly no. 5), with its 200-milligal local closures, is the maximum positive anomaly of the region. This anomaly abruptly comes to an end along a straight line in the west and following the southern coast of Cyprus extends to the Gulf of İskenderun, with nosing of contours and ends there on a line running in a N-S direction. The northern extension of this anomaly is less well defined. It extends with linear gradient until it is disturbed by the Taurus Mountain Range low in the north.

The linear northern gradient of the Cyprus Anomaly is also disturbed by a local gravity high at the Gulf of Silifke and a gravity low at the Gulf of Mersin. These gravity high and low, due to high gradient of Cyprus Anomaly, are only discernable on the map by undulations on the gravity contours. Better defined and similar disturbances in the linear gradient of the Cyprus Anomaly are seen over Adana area and the Gulf of İskenderun.

A further similar disturbance discernable by the undulations of contour lines is seen in south-east Anatolia, disturbing the linear southern gradient of Anomaly no. 4.

6. The Gulf of the Antalya Anomaly (Anomaly no. 6), with a broad 100-milligal closure, appears to be a natural continuation of the Cyprus Anomaly to the east. However it is observed with interest that, while the Cyprus Anomaly lies over land, Anomaly no. 6 lies over the Gulf of Antalya abyssal deep. Anomaly no. 6 abruptly ends at the Anatolian Coast line and apparently is disturbed by a disturbing mass over its northern extension which is discernable by very slight disturbance in the linear northern gradient of the Anomaly. Anomaly no. 6 is clearly separated from Anomaly no. 5 by the western limit of the Cyprus Anomaly along a straight line.

7. The gravity minimum (Anomaly no. 7) following the arc-like trend of the Taurus Mountain Range, with its two, 100-milligal closures, marks the northern limit of the Cyprus Anomaly.

This Anomaly, well defined by an 80-milligal contour line, following the arc-like trend of the Taurus Range and the eastern coast of Beyşehir Lake, extends to the Lake District in the west. The extension of Anomaly no. 7 in the Lake District is marked by the southward nosing of the contours of 90-milligal anomaly (Anomaly no. 9), in the Afyon Region. The E-W nosing of the Anomaly no. 9 at its northern border, suggests that Anomaly no. 7 may extend further to the north. Anomaly no. 7 extends with a broad nosing towards the south, due to the disturbing mass at the Gulf of Mersin.

8. To the north of Anomaly no. 7, a number of local gravity closures form the Tuz Gölü-Konya region anomaly zone (Anomaly no. 8). In general this zone forms a relative gravity maximum between Anomaly no. 9 and Anomaly no. 4 in the Afyon and Eastern Anatolia regions respectively. As the anomalies of this zone have been compiled from detailed gravity surveys, local anomalies are

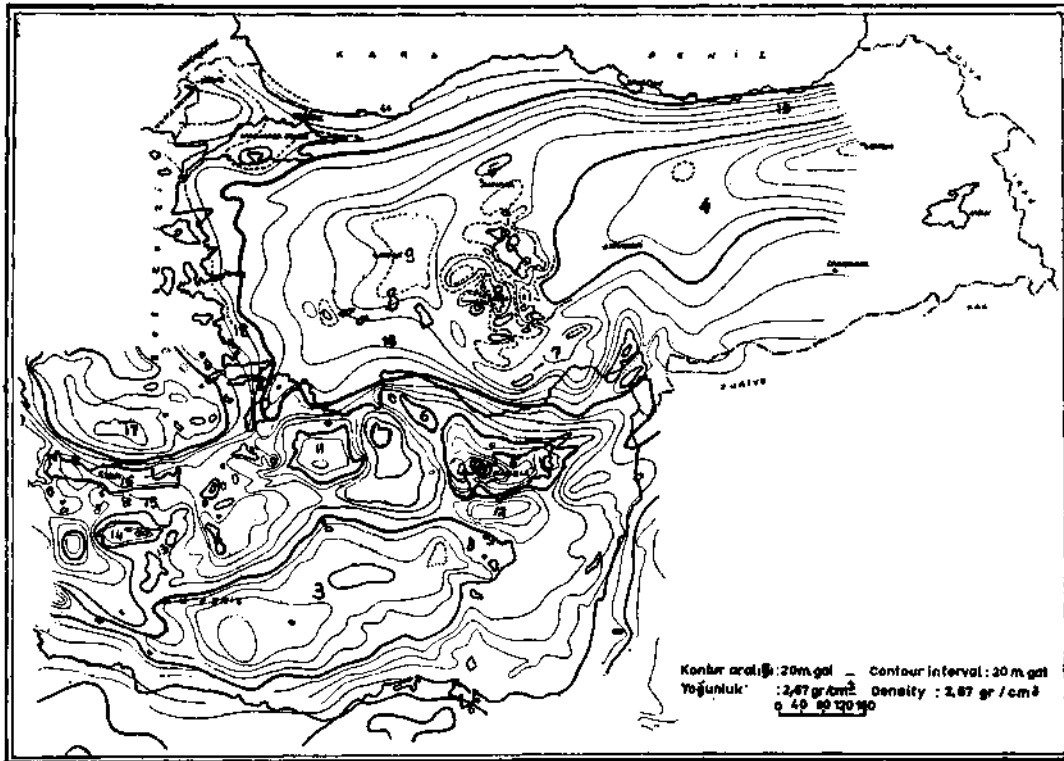


Fig. 1 - Eastern Mediterranean region Bouguer anomaly map.

better defined in this region. From these local anomalies, two tectonic zones are clearly discernable in this region: one in the south, characterized by N-S-trending linear contour lines and the other in the north, characterized by linear contours trending in NW-SE directions, parallel to the general tectonic trend of Tuz Gölü. An 80-milligal small closure to the north of Ankara appears to correlate well with the nosing of contours of Anomaly no. 9 in the Afyon region, that trends along the same direction.

9. Anomaly no. 9 in the Afyon region, with the nosing of contour lines at its SE and NW corners can be related to the Taurus Anomaly (Anomaly no. 7), while on the other hand it can be related to the narrow arc-like gravity minimum extending over Rhodes to Crete, by the nosing of contour lines at its NE and SW corners.

10. Anomaly no. 10 in the Lake District Region, with the northward nosing of low-gradient contour lines forms a weakly defined gravity maximum. This area appears to be the extension of the arc-like gravity maximum running directly south of the Crete minimum, over into Anatolia. This gravity maximum to the south of Crete includes some of the conspicuous gravity anomalies of the Eastern Mediterranean Basin.

11. A square-shaped gravity high of 140 milligals situated to the SE of Rhodes (Anomaly no. 11) occurs on the side of the Rhodes abyssal plane and constitutes one of the conspicuous anomalies of the arc-like gravity maximum running to the south of Crete. This anomaly is separated from the Gulf of Antalya Anomaly (Anomaly no. 6) by a gravity minimum marked by a zero contour line. It seems that this anomaly group extends over Anatolia to the Lake District as a relative gravity maximum. The fall in the gradient to the south of these anomalies and the nosing of contour lines suggest that the gravity minimum to the south of Cyprus (Anomaly no. 12) extends towards west.

12. Anomaly no. 12 forms a marked gravity minimum to the south of Cyprus. This minimum continues to the east along NE-SW direction, following -20-milligal gravity minimum and narrow nosing of zero contour line. Its extension to the west along the southern border of the gravity maximum running to the south of Crete is marked by the fall of gradient and nosing of contour lines. In the west, it extends to Anomaly no. 13.

13. Two gravity maximums of 100-milligal closure, striking in NE-SW direction form Anomaly no. 13. It is one of the conspicuous anomalies of the gravity maximum to the south of Crete. This anomaly forms the western limit of the gravity minimum to the south of Cyprus. To the east it is bordered by a narrow gravity minimum marked by a zero contour. The strike of the gravity minimum and the western gradient and linear contours indicate that this zone may be a fault zone extending beyond Crete to the north.

14. Anomaly no. 14 is another one of the conspicuous anomalies of the gravity maximum to the south of Crete. It is marked by 120-milligal closure and it strikes in E-W direction. To the west, like other gravity maximums in this zone, it is bordered by a gravity minimum marked by a zero contour.

15. Anomaly no. 15 is a narrow zone running parallel to the Cretan Arc between Crete and the gravity maximum to the south of Crete with conspicuous gravity maximums separated by gravity minimums marked by zero contours. This zone is characterized by very small gravity closures. This zone appears to extend from the south of Crete as far as Rhodes and disappears before reaching Anatolia.

16. Anomaly no. 16 is the gravity minimum over Crete. This minimum extends over Rhodes into Anatolia and continues over Afyon to Ankara. The extension of this minimum over Anatolia is marked by the undulations in the contour lines and by the 80-milligal closure to the north of Ankara.

17. The broad positive 160-milligal closure to the north of Crete is Anomaly no. 17. This zone is well known with its 150-milligal positive isostatic anomaly which is quite comparable with Cyprus. Some authors consider this zone as back deeps that are characteristic features of present-day island arcs. No evidence can be seen over Anatolia to suggest the extension of this zone. Although the broad undulations in the contour lines over Menderes Massif suggest the extension of this zone to this area, changes in gradient rule out this suggestion. The linear span of contours suggest that N-S striking faults prevail in this interesting zone. It is observed with interest that this suggestion conforms with the strike of the coastal lines of Crete too.

18. Anomaly no. 18 is the poorly defined Menderes Massif Anomaly. It is observed with interest that the contour lines to the south of İzmir diverge like a fan. Despite the closely spaced profiles and gravity observations in this region, this pattern would not change. Broad undulation of contour lines in this region suggest that over Menderes Massif a gravity high occurs.

19. Gravity anomalies in the north of Anatolia, due to very wide spacing of observations appear much smoother and no individual anomalies are discernable in this part. However there are some points of interest about the gravity anomalies in this region too. In the Eastern Black Sea Region the gravity gradient is very high and here the zero contour closely follows the coast line. As one goes to the west, however, the gradient noticeably falls down and the zero contour runs in the land areas. It is observed with interest that the whole of Marmara Sea and Thrace Basin have positive Bouguer anomalies. It is also observed that the Thrace Basin with very thick sediments could only be marked by a very feeble gravity minimum but with positive values.

With respect to the general characteristics of the gravity anomalies, the Eastern Mediterranean Region may be subdivided into the following gravity anomaly zones (See Fig. 2):

1. The broad, 160-milligal gravity closure to the north of Crete (Zone 1).
2. The gravity minimum over Crete extending over Rhodes to Afyon and to Ankara in Anatolia (Zone 2).
3. A narrow zone characterized by very small gravity closures to the south of Crete (Zone 3).
4. A broad gravity maximum to the south of Zone 3, with conspicuous 100-milligal anomalies separated by gravity minimums marked by zero contours (Zone 4).

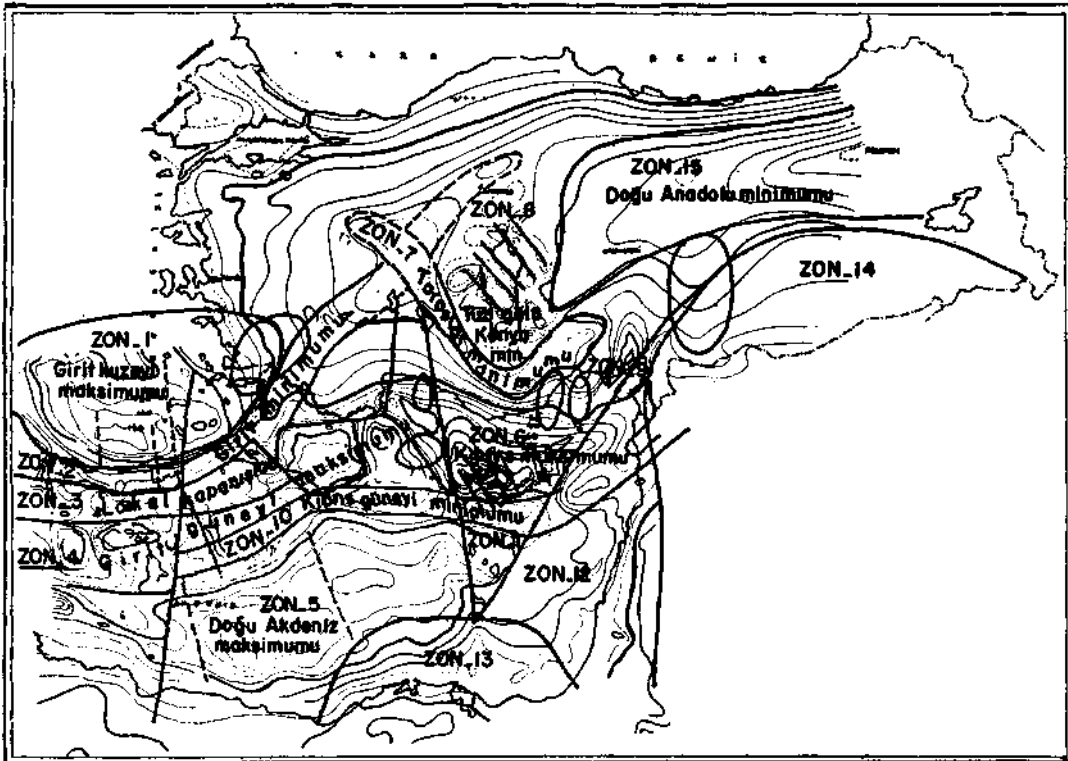


Fig. 2 - Eastern Mediterranean Bouguer anomaly zone map.

5. The broad 160-milligal gravity maximum covering a large part of the Eastern Mediterranean Basin (Zone 5).
6. Cyprus Anomaly Zone (Zone 6).
7. Taurus Mountain Range Gravity Minimum Zone (Zone 7).
8. Tuz Gölü-Konya Region Anomalies. Zone (Zone 8).
9. Adana-Gulf of İskenderun and Silifke-Gulf of Mersin Anomalies Zone (Zone 9).
10. Gravity minimum to the south of Cyprus and its extension zone (Zone 10).
11. A zone characterized by very small gravity closures to the south of Zone 10 (Zone 11).
12. A very low gradient zone to the east of Zone 11 (Zone 12).
13. Nile Delta Zone (Zone 13).
14. Border Fold Zone (Zone 14).

15. Eastern Anatolia Gravity Minimum Zone (Zone 15). This zone may be divided into two zones:

- a. Kayseri Zone with low gradient.
- b. Erzurum Zone with higher gradient

THE GRAVITY ANOMALIES AND TOPOGRAPHIC ELEVATION RELATIONS

The inverse relation between gravity anomalies, and the topographic elevations in some parts of the Eastern Mediterranean Basin has been observed previously by Harrison (1955). In this thesis it has been determined that this inverse relation is also valid for Anatolia.

The inverse relation between gravity anomalies and topographic elevations over the oceans is determined by having low positive gravity anomalies over ocean deeps and larger gravity anomalies over shallower zones. Over land areas the same relation is determined by lower negative anomalies over elevated ground than would be expected under normal isostatic conditions or with a positive linear correlation coefficient for gravity versus elevation graph.

In Figure 3, the Eastern Mediterranean Basin Bathymetric Map is shown. A comparison of this map with the Bouguer Anomaly Map shown in Figure 1 readily shows the following gravity anomaly-elevation relations:

1. The maximum value of Anomaly no. 17 occurs over the shallow zones rather than deep zones. Deeper zones over 1000-meter depth have not given any noticeable anomalies.
2. While there is no gravity anomaly over the Pliny Trench, Anomaly no. 14 occurs over a similar depth zone and extends on to shallower areas.
3. While the Rhodes Abyssal Plain with its 2000-meter depth does not give rise to a noticeable anomaly, to the south of this zone, Anomaly no. 11 occurs over a shallow zone.
4. It is observed with interest that Anomaly no. 6 only partly occurs over the Antalya Abyssal Plain and extends further over the shallow zones, striking in a different direction than the Antalya Abyssal Plain.
5. The trench south of Cyprus forms a relative gravity minimum with respect to the Cyprus Anomaly (no. 5) and Anomaly no. 3 despite its greater depth.

All the above examples show that the gravity anomalies of the Eastern Mediterranean Basin, with inverse relation with elevation, cannot be explained by normal mantle-crust relations.

Normally over land areas it is expected that Bouguer anomalies get larger negative with increase in elevation. The Eastern Mediterranean Region shows inverse conditions in this respect too.

A study of Figure 1 readily shows the following inverse relations:

1. The Cyprus anomaly being over a land area should normally be negative. With its positive 200-milligal value it forms a very good example for the inverse relation.
2. It is observed with interest that the Aegean Islands give positive gravity anomalies. Normally they should be negative, being over land areas.
3. Under normal conditions, zero Bouguer anomaly contour should follow the coast lines. It is observed with interest that the zero contour in Figure 1 runs in part over land areas. A good example for the prevalence of inverse conditions in the region.



Fig. 3 - Eastern Mediterranean bathymetric map.

4. In Anatolia, the Adana Plain-Gulf of İskenderun and the Silifke - Gulf of Mersin anomaly couples being positive over land areas and negative over sea areas provide interesting examples for the inverse relation.

5. Under normal isostatic conditions where compensation prevails, an empirical relation between average- elevation and average Bouguer anomaly can be obtained (Wollord, 1962). In the Kayseri zone of the Eastern Anatolian gravity minimum (Anomaly no. 4), where average elevation is 1000 meters, it is normally expected to have minus 200-milligal Bouguer anomaly. However it is observed with interest that in the zone, the average Bouguer anomaly has been found to be minus 100 milligals, with an excess of 100 milligals. In the Erzurum zone of the same anomaly where the average elevation is 2000 meters, average Bouguer anomaly value has been obtained minus 200 milligals with the same excess of 100 milligals.

6. In the Konya - Tuz Gölü region where average elevation is 900 meters, average Bouguer anomaly value has been determined to be minus 70 milligals with the same excess of 100 milligals. It has been also determined that a similar condition is also true for the Afyon region.

All the above examples show that inverse relation between elevation and gravity anomalies prevail over Anatolia too.

It is also observed with interest that the 100-milligal difference between the Eastern Mediterranean Basin and other oceans is also true for Anatolia and other isostatically compensated regions of the world. Another point which is observed with interest is that when 80 milligals is subtracted from the gravity values over Anatolia, the zero Bouguer anomaly contour will follow the coast line. This last observation also indicates the presence of an 80-100-milligal excess gravity value over Anatolia.

In this thesis, the gravity anomaly-elevation relations in Anatolia have been investigated by analyzing the linear correlation coefficient and regression line relation of gravity and elevation value taken along profiles.

The results of this investigation may be summarized as follows:

1. In Graphs no. I, II and III, linear relations between elevation and the three gravity values, namely gravity values with latitude correction, free-air anomaly and Bouguer anomaly calculated for 2.67 density are shown respectively.

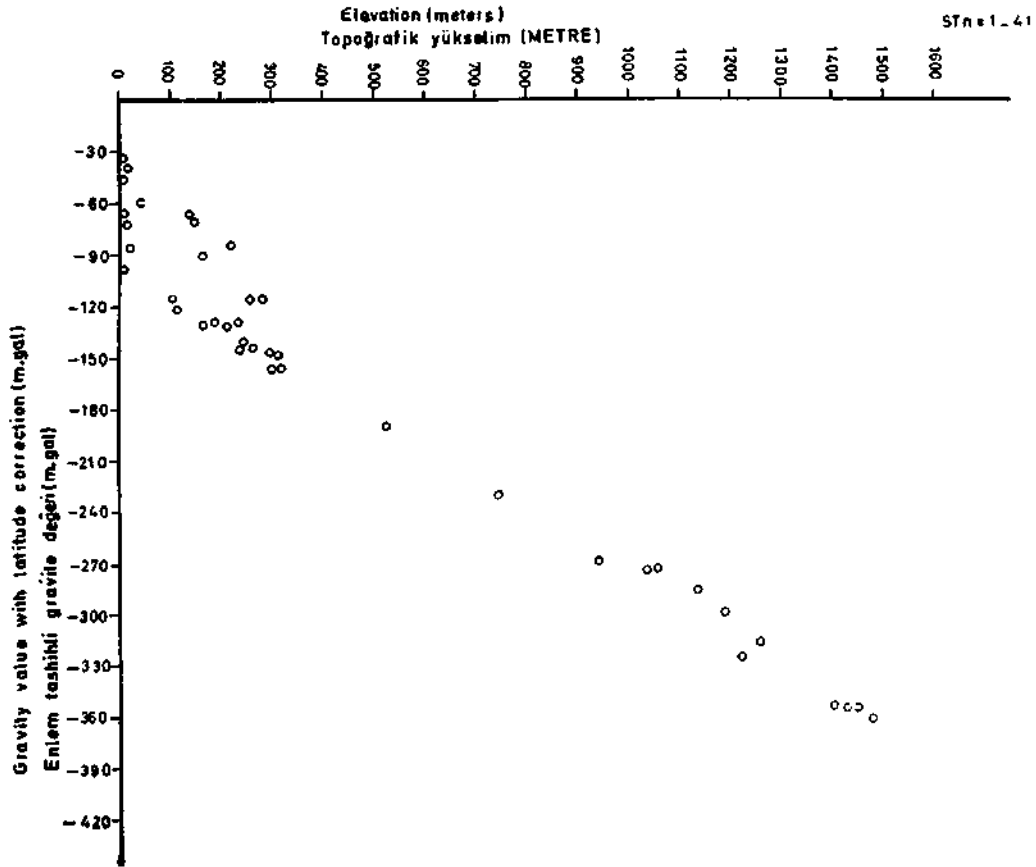
In these graphs, results for gravity stations from 1 to 48 are shown; it is observed with interest that for the three values of gravity, there exists a good linear relation.

To analyze the statistical linear correlation, linear correlation coefficients for the three values of gravity were calculated with a computer and they were found to be -0.982 , -0.938 and $+0.154$ for gravity values with latitude correction, free-air anomaly and Bouguer anomaly respectively.

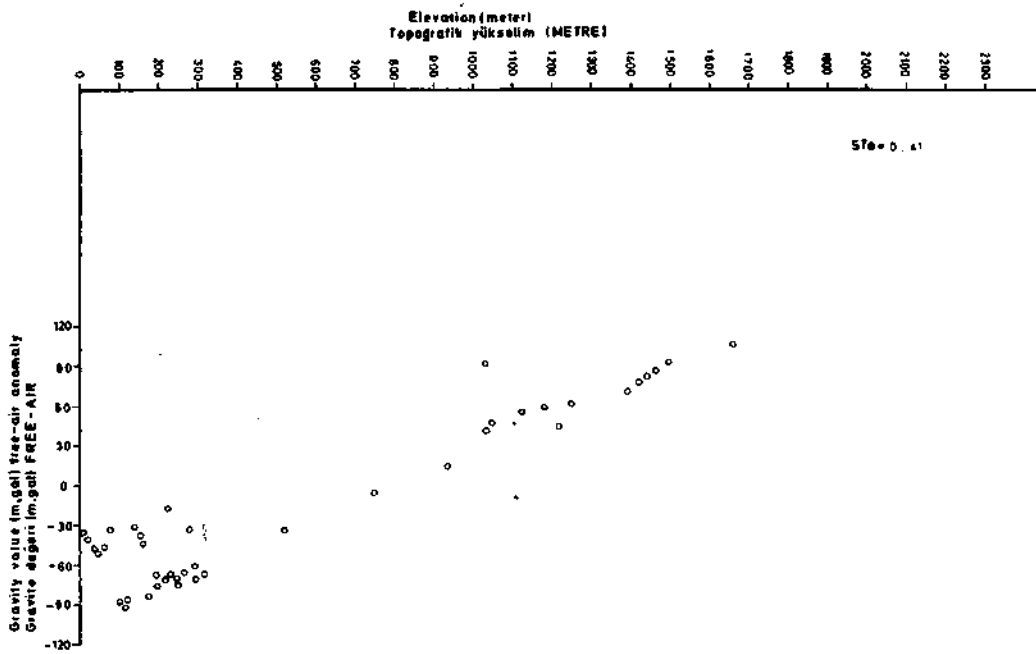
As it would normally be expected, the first two correlation coefficients being very near unity, indicate a perfect statistical correlation.

However, the third correlation coefficient being very low, indicates no statistical correlation between Bouguer anomaly values and elevation, despite the fact that in the graph there exists a good linear relation between the two quantities.

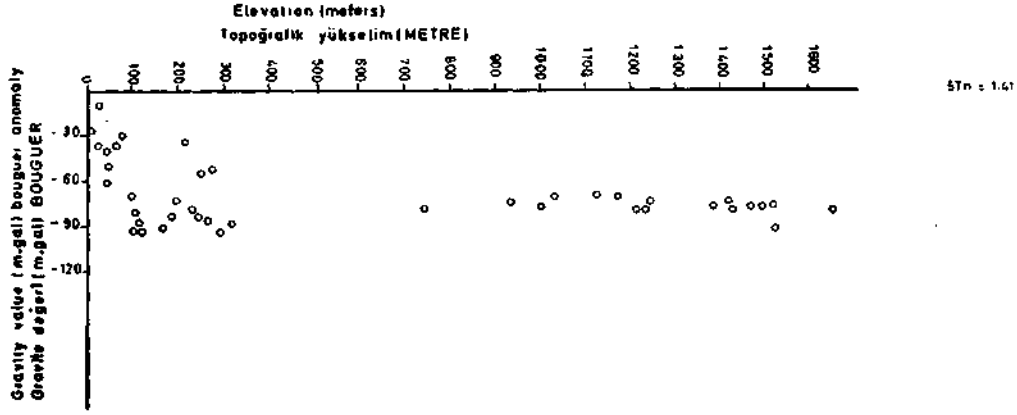
In Graph no. III, for high elevation values, a positive correlation is readily seen between Bouguer anomaly and elevation values. It is also observed with interest that due to the low slope of the regression line and due to the scatter of gravity values at low elevations, the correlation coefficient for Bouguer anomalies has been found to be very low.



Graph I - Taurus region gravity value-elevation graph.



Graph II - Taurus region free-air anomaly elevation graph.



Graph III - Taurus region Bouguer anomaly-elevation graph.

Existence of perfect statistical correlation between Bouguer anomaly and elevation has been demonstrated by calculating linear correlation coefficient for gravity stations 1 to 33, excluding gravity stations with low elevation. In this calculation correlation coefficient was found to be 0.81578, very near unity, indicating perfect statistical correlation between the two quantities.

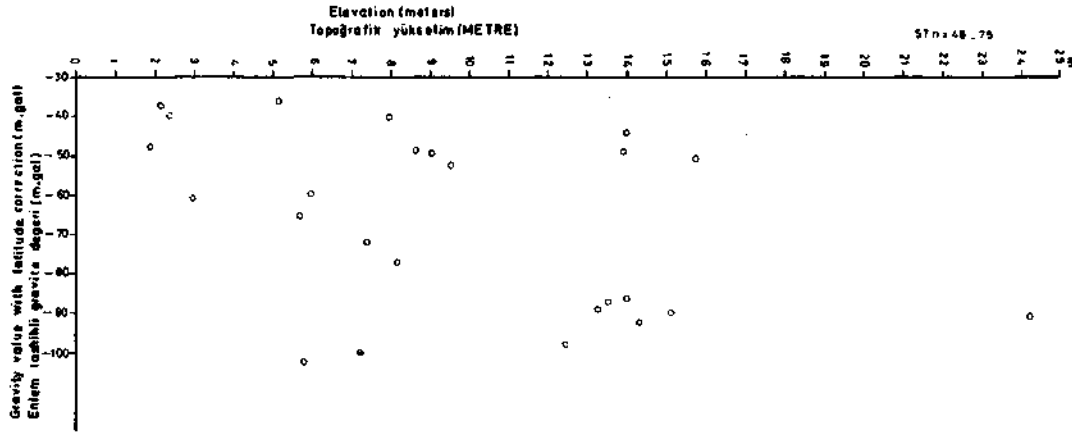
Normally it is expected that Bouguer anomalies should have no correlation with elevation, and if there is a correlation, it should at least be negative.

In our case, having found a perfect positive linear correlation the correlation forms a very good example for inverse relation between gravity values and elevation in the region.

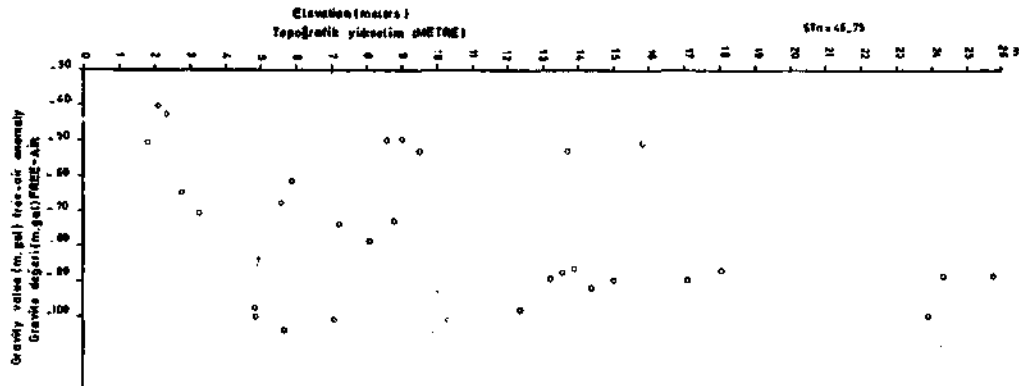
2. In Graphs no. IV, V and VI linear relations between the same gravity values and elevation are shown for gravity stations 48 to 75. The stations having low elevations, gravity values show no relation to elevation in all three cases. The linear correlation coefficients calculated for the three gravity values were found to be -0.464 , -0.383 , -0.297 , indicating no statistical correlation between the two quantities.

Normally a perfect negative correlation between elevation and gravity values with latitude correction and a perfect positive correlation between elevation and free-air anomaly values and no correlation or negative correlation between elevation and Bouguer anomaly values are expected. As no such correlations can be seen in the Graphs no. IV and V, the importance of the effect of low elevations in correlation analysis is well demonstrated with these examples.

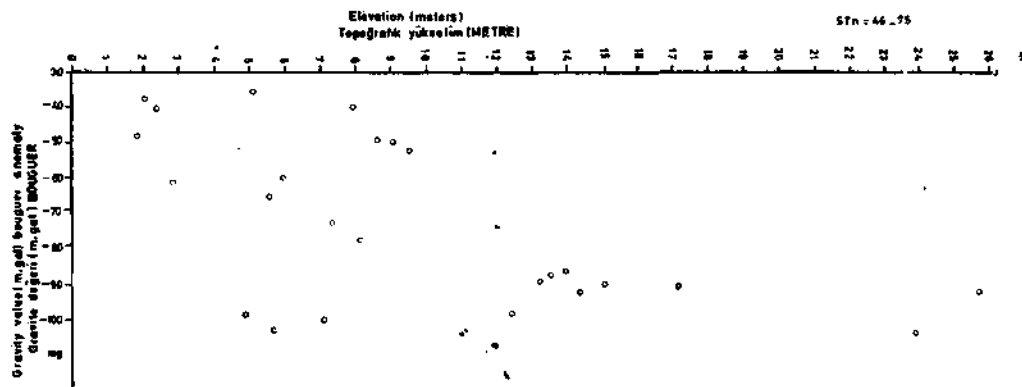
3. In Graphs no. VII, VIII and IX the same relations are shown for gravity stations 75 to 105, with considerable elevation variations. In these graphs a good linear relation is seen between the two quantities for the three values of gravity. Linear correlation coefficients calculated for the three gravity values were found to be -0.985 , 0.939 and -0.266 respectively. As it would normally be expected, gravity value with latitude correction and free-air anomaly values have perfect negative and positive statistical correlations respectively. However Bouguer anomaly values having very low



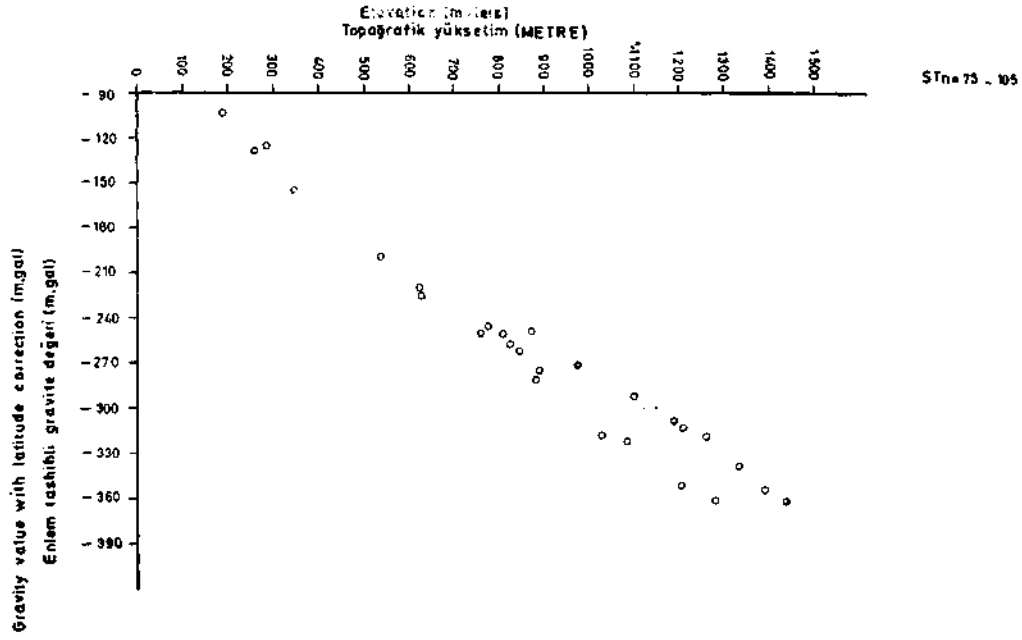
Graph IV - Taurus region gravity value-elevation graph.



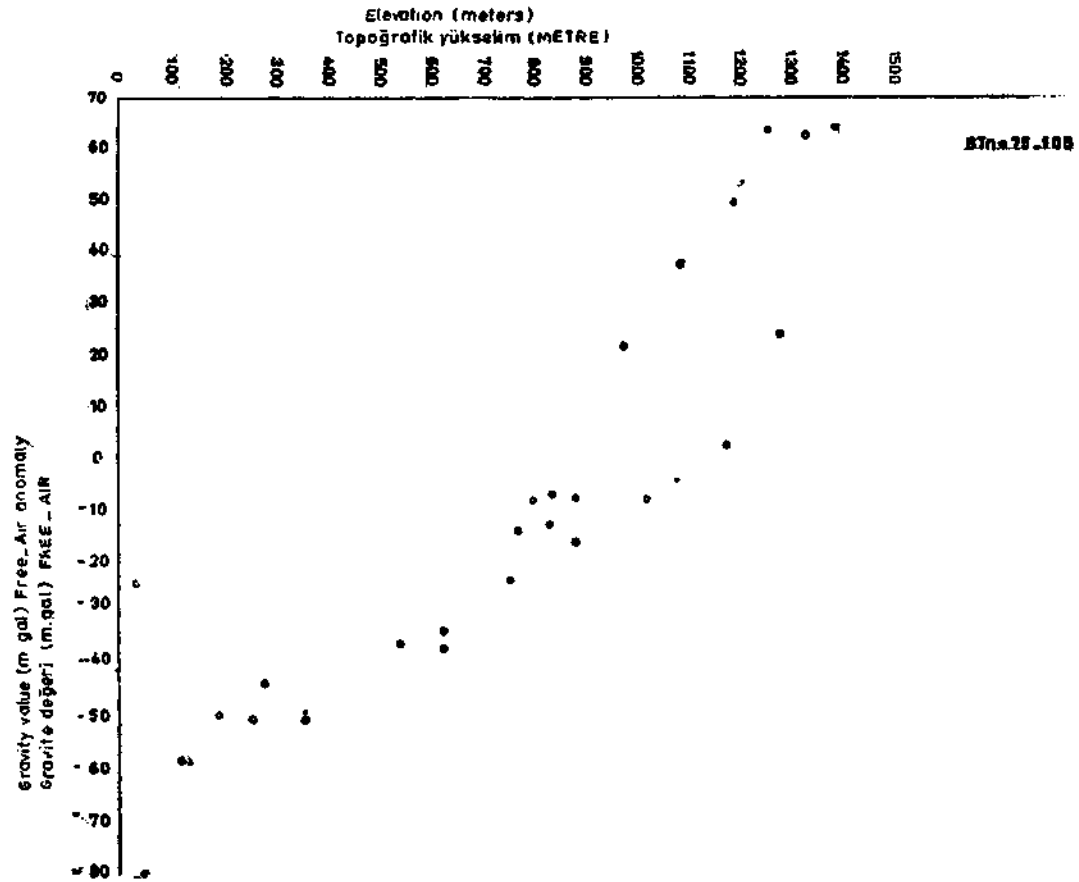
Graph V - Taurus region free-air anomaly-elevation graph.



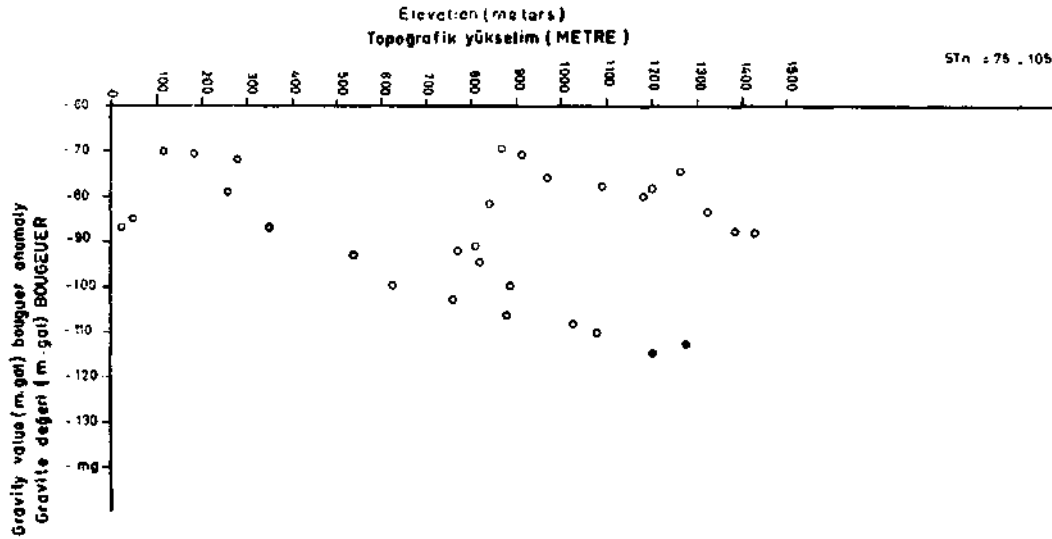
Graph VI - Taurus region Bouguer anomaly-elevation graph.



Graph VII - Taurus region gravity value-elevation graph.



Graph VIII - Taurus region free-air anomaly-elevation graph.



Graph IX - Taurus region Bouguer anomaly-elevation graph.

correlation coefficient have no statistical correlation with elevation. In Graph IX, very good linear relation with elevation and Bouguer anomaly values is readily seen and it is observed with interest that this situation arises from the scatter of points in the interval taken for calculations. It is also observed with interest that in this example the correlation coefficient for Bouguer anomaly values is negative and therefore indicates a normal relation between gravity values and elevation.

4. To eliminate the effects of low elevation and scatter of values in large intervals, narrower intervals and stations with higher elevations were used in linear correlation coefficient calculations and the following results were obtained;

Interval (station)	Correlation coefficient		
	Gravity value	Free-air anomaly	Bouguer anomaly
1 - 33	- 0.99815	0.99623	- 0.81578
34 - 46	- 0.95478	0.38105	- 0.76586
77 - 89	- 0.99805	0.97313	- 0.94718
90 - 95	- 0.99804	0.95193	- 0.78998
96 - 105	- 0.99538	0.98428	- 0.89145

These results show clearly that there is a perfect statistical correlation with the three values of gravity and elevation. The physical meaning of this may be stated that the elevations are related with mass distribution or with deep geological structures.

The positive correlation coefficient calculated for stations 1 to 33 for Bouguer anomaly values indicates that in this region, elevation is related with heavier mass, the configuration of which closely fits the topographic configuration.

Correlation coefficients calculated for Bouguer anomaly values in other intervals being negative, indicate that the elevation is related with deficiency of mass, the configuration of which closely fits the topographic configuration.

According to the concept of isostasy, the first relation forms an inverse relation between gravity and elevation and the second relation a normal relation.

5. In Figure 4, a perfect but inverse relation between elevation and gravity values is seen along the Silifke-Karaman gravity profile. In the figure, Bouguer and free-air anomaly values are shown with the topographic section. It is seen with interest that Bouguer anomaly values in contrast to normal conditions are increasing with the increase in elevation.

6. In Figure 5, a Bouguer anomaly profile in the Orhaneli region is shown with topographic variations and geological cross section. The profile has been taken between Orhaneli and Dağakça. In the profile, a very good correlation with the geological formations and the undulations on the

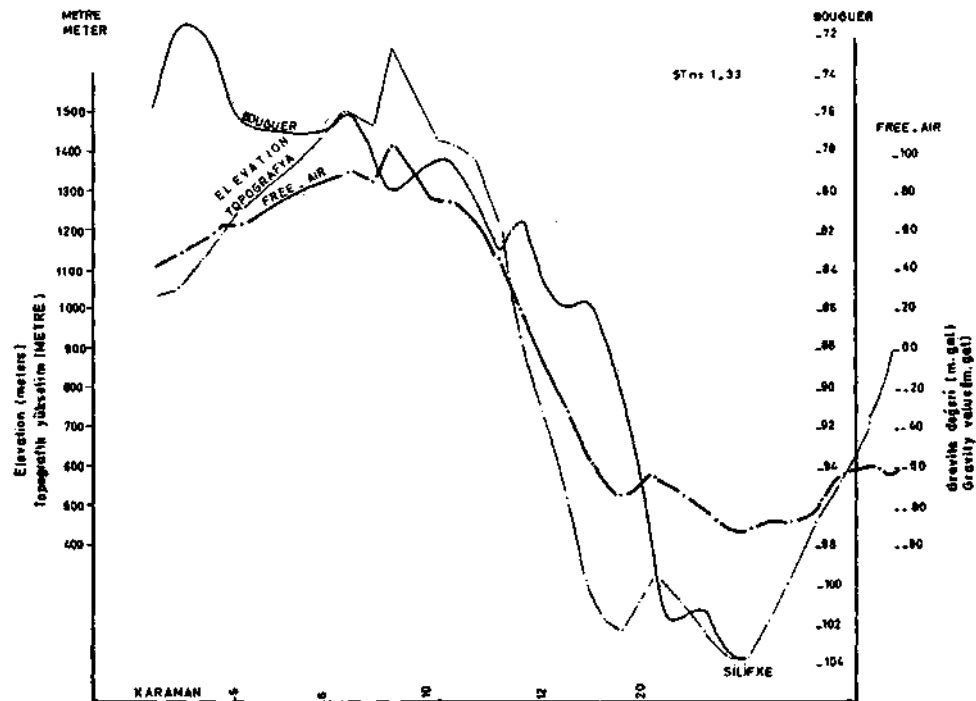


Fig. 4 - Bouguer free-air and elevation profile between Karaman and Silifke in Taurus region.

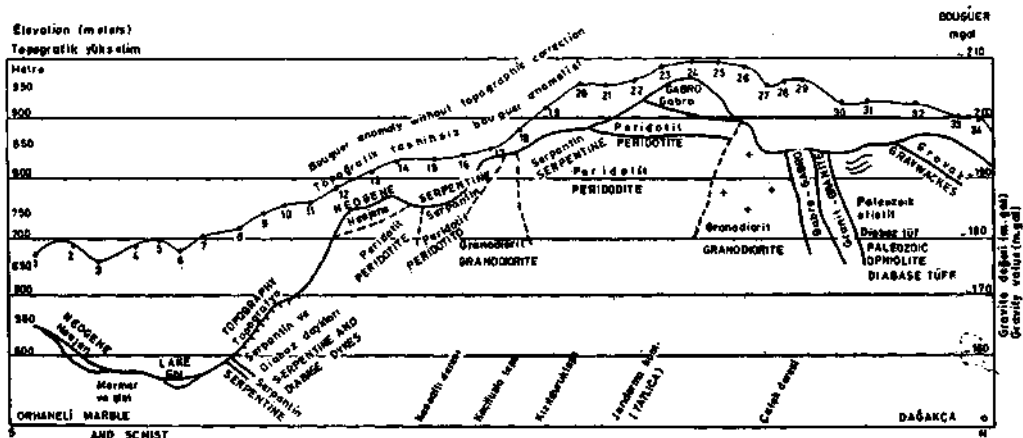


Fig. 5 - Gravity profile between Orhaneli and Dağakça.

gravity anomaly values along the profile is seen. In general, however, the gravity value variations along the profile cannot be related to geological formations, but they are clearly related with the topographic elevation variations. Parallelism of the gravity profile with the topography is strikingly good. This suggests that the broad gravity anomaly is related to deep-seated structure and topographic elevation is an expression of this structure. It also suggests that the variety of geological formations seen at the surface are not deep-seated but only superficial expressions of a deep-seated tectonic unit.

A negative correlation coefficient is clearly seen between elevation and Bouguer anomaly values. This indicates a deficiency of mass, the configuration of which closely follows the topography, and a normal relation between gravity values and elevation. The linear correlation coefficient calculated for gravity values with latitude correction and gravity values with latitude and topographic corrections were found to be -0.943 and -0.941 respectively, which indicates perfect statistical correlation between the two quantities.

7. In Figure 6, another gravity profile in the Orhaneli region, taken between Manastir Tepe and Erenler, is seen with topographic and geological cross sections. In this profile a good correlation is seen between Bouguer anomalies and elevation and also with faulted blocks.

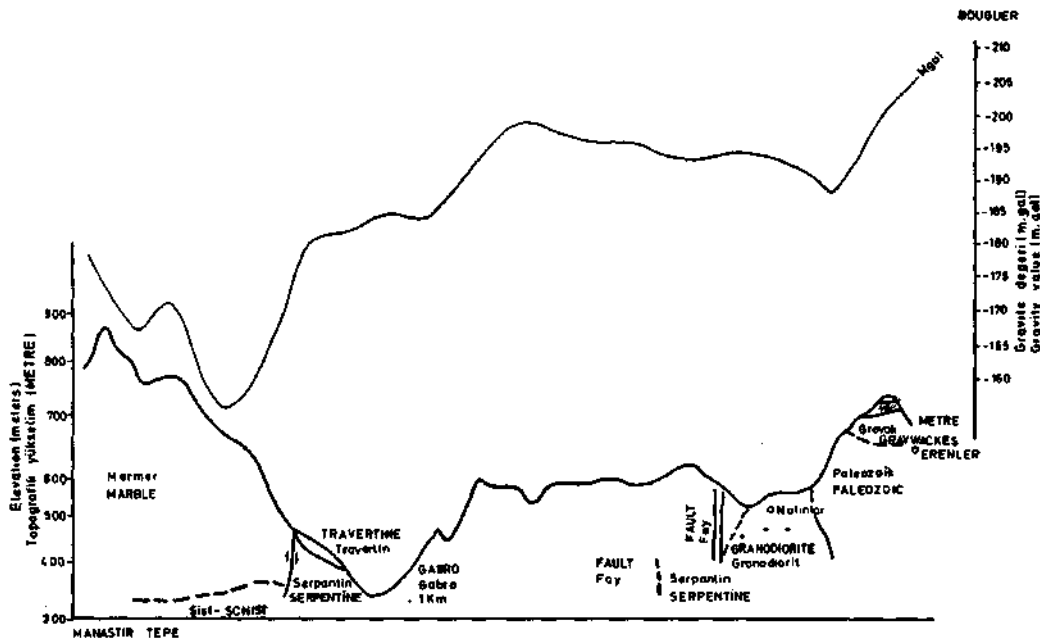


Fig. 6 - Gravity profile between Manastir Tepe and Erenler.

To the left of the profile, an over 500 meters thick marble zone gives higher gravity value than gabbro and serpentine formations to the right, despite the negative density contrast. It is clear from this observation that gravity anomalies in general cannot be related to surface geology but they are related with deep-seated structure.

In the profile, decrease in Bouguer anomaly values with increase in elevation is observed, indicating a normal relation between gravity values and elevation. However, it is also observed that the highest elevation does not correlate with the lowest Bouguer anomaly. Although the highest elevation area along the profile lies over the low density marble formation, the gravity value in this area is nearly the same as that measured over serpentine and gabbro formations at much lower elevations.

This indicates a possibility of inverse relation between gravity values and elevation. Linear correlation coefficients for this profile are not calculated.

8. In Graphs X, XI, XII and XIII, the relation between gravity values and elevation for profiles over the Taurus Mountains is shown for gravity values with latitude correction. In these graphs all gravity stations over the Taurus Mountains from 1 to 105 are shown.

Gravity values with latitude corrections include gravity effect due to elevation variations which are normally corrected for in the calculation of Bouguer anomalies. These effects are the free-air effect and Bouguer effect. Both effects have a perfect linear correlation with elevation.

In Graphs X, XI, XII and XIII, the gravity value with latitude correction and its relation with elevation is compared with the normal free-air effect and Bouguer effect calculated with density 2.67. Comparison is also made with elevation effect which is normally the combination of the first two effects.

It is observed with interest that the linear relation between gravity value with latitude correction and elevation was in some parts perfectly parallel to the normal free-air effect, in some parts perfectly parallel to the normal Bouguer effect and in other parts, perfectly parallel to the normal elevation effect.

To analyse this property statistically, regression coefficients and intercepts of regression lines were calculated from the linear correlation coefficients.

Equation of regression line may be expressed with the following equation of a straight line:

$$y = ax + c \quad (1)$$

where:

y = gravity value with latitude correction
 a = regression coefficient
 x = elevation
 c = intercept

Equation (1) may also be written in the following way:

$$c = y - ax \quad (2)$$

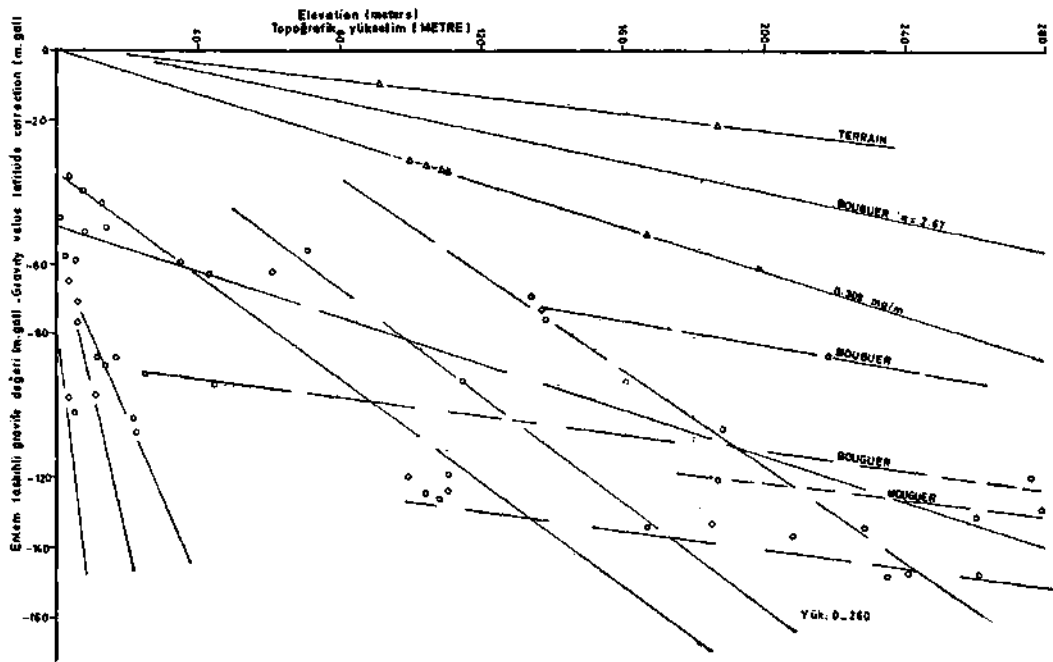
From equation (2), it is readily seen that c , intercept, is statistically the average Bouguer anomaly for the region but without topographic correction; and a , the regression coefficient, is the elevation correction constant.

From the analysis of regression coefficients and the intercept of regression line, the following results were determined:

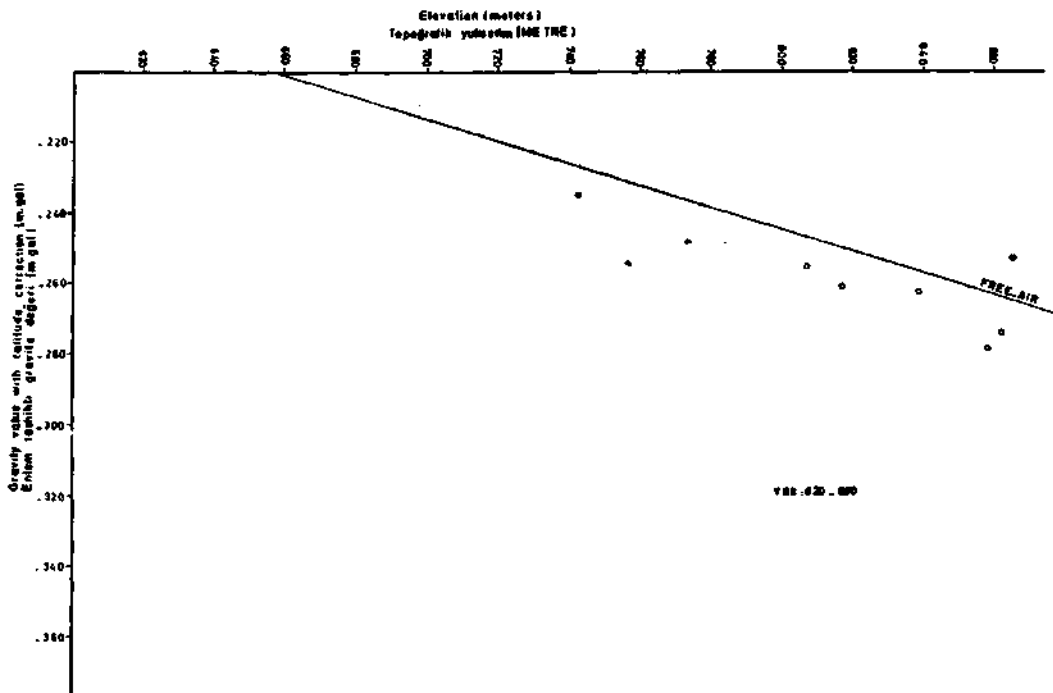
a. Normally the elevation correction constant for 2.67 density should be 0.1968 milligals/m.

The regression coefficients and intercept values found from the analysis were as follows:

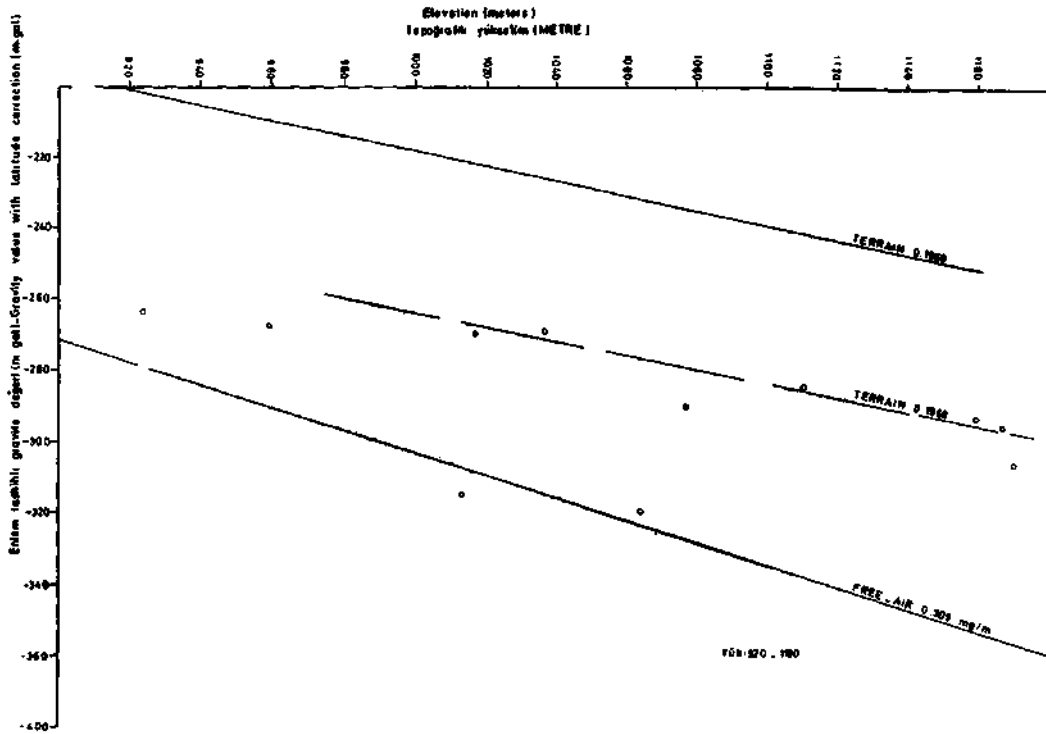
<i>Interval gravity station</i>	<i>Regression coefficient</i>	<i>Corresponding density</i>	<i>Intercept</i>	<i>Average elevation</i>
1 - 33	— 0.181	3.08	— 100.88	687
34 - 46	— 0.273	0.90	— 41.50	108
47 - 76	Due to low elevation variations no correlation could be determined.			
77 - 89	— 0.224	2.0	— 68.53	622
90 - 95	— 0.259	1.2	— 49.90	863
96 - 105	— 0.200	2.6	— 80.78	1157
1 - 46	— 0.202	2.5	— 75.43	524
47 - 75	Due to low elevation variations no correlation could be determined.			
76 - 105	— 0.209	2.4	— 83.77	830



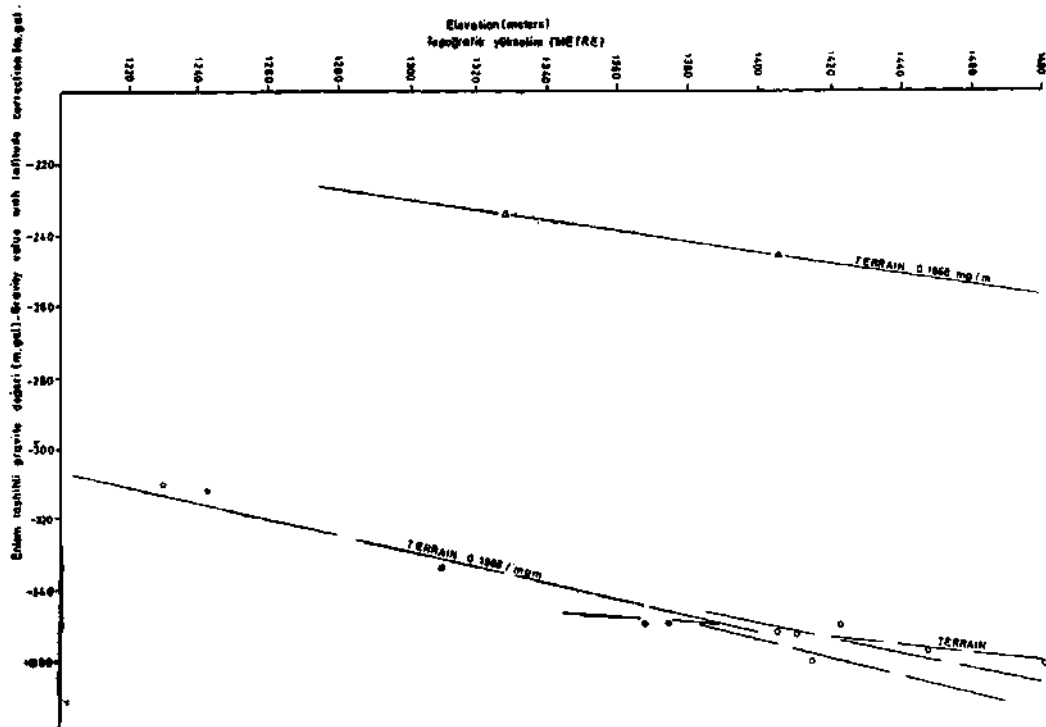
Graph X - Taurus region gravity value and elevation graph.



Graph XI - Taurus region gravity value and elevation graph.



Graph XII - Taurus region gravity value and elevation graph.



Graph XIII - Taurus region gravity value and elevation graph.

From these results it is readily seen that regression coefficients calculated from correlation coefficients are considerably different from the elevation correction constant.

This may be due to a linear relation present between Bouguer anomaly values and elevation or it may be due to different density of crust in this region than 2.67 gm/cm^3 commonly used for gravity reductions, or it may be due to variation of free-air correction constant in the region.

Normally Bouguer anomaly values are expected to have no linear relation with topographic elevation unless the topography is actually related with the anomaly causing mass. If the differences found in the results are related to the linear relation between Bouguer anomaly values and elevation, they are observed with interest as they indicate that the topography is related with the geological structure causing the anomaly.

Elevation correction is the algebraic sum of the free-air correction and Bouguer correction. Normally as the free-air correction is constant, the difference between the regression coefficients and the normal elevation correction constant may arise from the difference of crustal density used in Bouguer correction calculations. In the third column, corresponding densities for regression coefficients are given. It is observed with interest that the difference in regression coefficients and elevation correction constant cannot be eliminated by the change of density in the practical limits. This leaves us with looking at the cause of the differences, in the variation of free-air correction constant. The developments in the last few years indicate that the free-air correction constant varies from place to place over the world and this variation is due to local geological conditions. Recent developments indicate that in the mantle there are zones of low velocity which may be related with phase changes in the mantle. These zones may cause a considerable variation in the vertical gradient of gravity values which in turn will cause variations in the free-air correction constants.

b. From regression coefficient analysis, average Bouguer anomalies were calculated from intercept of regression line. In the fourth and fifth column of the analysis results, average Bouguer anomalies calculated from intercept and corresponding average elevations are shown respectively. A comparison of average Bouguer anomalies with the corresponding average elevations readily shows the inverse and normal gravity values and elevation relations.

Bouguer anomaly values being negative in general and as they generally fall with the increase in elevation, computed correlation coefficients were found to be negative for most cases, indicating normal relation between gravity values and elevation. However comparison of average Bouguer anomaly values with corresponding average elevation indicates that the gravity value elevation relations are in general inverse.

9. To analyse statistically the effect of local anomalies and the computed regression coefficients, intercepts and regression coefficients for free-air and Bouguer anomalies were also calculated.

A, O and X being intercepts for gravity values with latitude correction, free-air anomaly and Bouguer anomaly values respectively, they should all give the same average Bouguer anomaly value for the region in consideration.

Y, Y_1 and Y_2 being regression coefficients for gravity values with latitude correction, free-air anomaly and Bouguer anomaly values respectively, Y, Y_1 and Y_2 will be the elevation correction constant, Bouguer correction constant and the linear correlation coefficient constant between Bouguer anomaly values and elevation respectively.

Algebraic differences of these will then be:

$$Y - Y_1 = \text{free-air correction constant}$$

$$Y - Y_2 = \text{elevation correction constant}$$

$$Y_1 - Y_2 = \text{Bouguer correction constant}$$

Analysis results show that average Bouguer anomaly values determined from the three intercepts are not different from one another and the correction constants calculated from regression coefficients are not different from the correction constants used in gravity anomaly calculations. This was a good verification of the soundness of the analysis and it was proved thus, the effect of local anomalies and topographic effects to the analysis results were negligible.

10. In the analysis, ratios of regression coefficients were also calculated but no meaningful relation could be derived from these results.

11. Linear correlation coefficient, regression coefficient and average Bouguer value and average elevation correlation analysis in the gravity profiles over the Taurus Mountains indicate that inverse gravity-elevation relation in Eastern Mediterranean Basin continues over Anatolia too. This in turn indicates that the gravity anomalies are caused by the rising or downwarping of mantle together with the crust as seen in the elevation variations on the surface.

12. Large differences between the regression coefficients and the normal elevation correction constant indicate the presence of an asthenosphere or a low-velocity zone in the mantle in this region.

GRAVITY ANOMALIES AND ISOSTATIC RELATIONS

In the interpretation of gravity anomalies of the Eastern Mediterranean Region, one of the most important questions which should be considered is the inverse relations between the anomalies and the normal isostatic conditions.

Isostatic conditions as observed from gravity anomalies imply overcompensation where isostatic anomalies are negative and undercompensation where isostatic anomalies are positive. Where isostatic anomalies are zero it implies that the region is perfectly compensated.

Normally isostatic conditions require the rising of overcompensated regions and sinking of undercompensated regions where crustal rigidity is not sufficient to support the excess mass and stable blocks in compensated regions. In the Eastern Mediterranean Region it is observed with interest that these conditions are completely reversed locally and generally.

In general:

1. The Eastern Mediterranean Basin, having 100-milligal lower gravity value than other isostatically compensated oceans, it is in general overcompensated. Normally the Eastern Mediterranean Basin should rise under its present isostatic condition. It is known, however, that the Eastern Mediterranean Basin with its thick sediment-filled basins is actually sinking.

2. Anatolia, having 100 milligals higher gravity values than other isostatically compensated zones of the world, is in general undercompensated. Normal isostatic conditions require that Anatolia should sink. It is known, however, that Anatolia, with the exception of local grabens, is rising.

Locally:

3. Cyprus with its high positive Bouguer anomaly is undercompensated. Normal isostatic conditions require that Cyprus should sink. However it is known that Cyprus is rising.

4. The Silifke zone with its positive gravity anomaly should be undercompensated and it is known that this zone has risen 900 meters since Miocene time and it is still rising. Under normal isostatic conditions it is expected to sink.

5. The Menderes Massif, with its positive gravity anomaly is undercompensated. Under normal isostatic conditions it is expected to sink. With its graben structures, prevailing tension conditions indicate that this zone is actually rising.

6. The Adana Plain-Gulf of İskenderun anomaly couple the first one with its positive anomaly is undercompensated and the second one with its negative anomaly over sea area is overcompensated. It is known that the two zones are sinking where under normal isostatic conditions, the Gulf of İskenderun should rise.

It is obvious that the above isostatic movements in the region cannot be explained by normal mantle - crust relations. To explain upward movements of zones with positive gravity anomalies, an upward force in the mantle should be accepted. The developments in recent years show that such upward force in the mantle can be produced by phase changes which produce volume increase in the mantle.

While phase changes in the mantle can explain upward movements in undercompensated zones, the downward movements in zones which are overcompensated cannot be explained by this phenomenon if normal isostatic conditions are assumed to prevail in the region. However the presence of an asthenosphere in the region can explain both the upward and downward movement. Assuming that the asthenosphere has upwarped the crust under prevailing tectonic stress conditions to produce tension conditions, which in turn will produce graben formations where blocks sink into low-density asthenosphere to produce negative gravity, anomalies reflecting the general low-density of the asthenosphere, overcompensated zones and their downward movement can thus be explained, whereas crustal blocks up-pushed with the asthenosphere under tectonic compressional stresses explain the upward movement of undercompensated zones.

INTERPRETATION OF GRAVITY ANOMALIES

Gravity anomalies being a potential problem, they lack uniqueness in their interpretation. For this reason, any interpretation based on gravity data alone will only be one of the many solutions that can explain the same anomaly. In such interpretations, the most important thing that should always be observed is the conformity of the interpretation with other related phenomena.

The basic difficulty in the interpretation of the gravity anomalies in the Eastern Mediterranean Basin is the lack of deep seismic information which would provide the most important parameter, the thickness of the crust in the zone.

Deep seismic work carried out by Russians in the Ukraine, indicates that the crust in that zone has highly variable thickness and that the thickness of the crust varies in large proportions in very short distances. In the Eastern Mediterranean Basin and in Anatolia no such information is available. From the available literature it is understood that the complexity of the geology of the Eastern Mediterranean Basin inhibits such deep seismic work.

Interpretation of gravity anomalies based on sediment thickness variations or crustal thickness variations, in an area where crustal thickness is unknown, can only be one of the many solutions for the cause of the gravity anomalies, but they cannot be claimed to be the final and unique solution. From the available literature it is seen that the Eastern Mediterranean Basin gravity anomalies are related either with sedimentary thickness variations or crustal thickness variations. It is observed with interest that such interpretations fall short in explaining the general characteristics and inverse elevation relations of gravity anomalies and strange isostatic conditions seen in the area.

In the light of these strange gravitational conditions in the area, the interpretation of the gravity anomalies of the Eastern Mediterranean Region and the supporting evidence may be summarized as follows:

1. Interpretation of gravity anomalies based on the variations of thickness of sediments cannot be reconciled with the following facts:

a. The Eastern Mediterranean Basin isostatic anomalies suggest that this zone is overcompensated with the exception of Cyprus, the Nile Delta, the Aegean Sea, and the Cretan Arc back deep. The same region is characterized with 100-milligal lower gravity anomaly than other oceanic areas. These conditions cannot be accounted for by variations in the sedimentary thicknesses.

b. The Nile Delta with its thick sediment cover is characterized by a positive isostatic anomaly in contrast to the other areas of the zone, indicating that the rigidity of the crust in this zone is such that thick sediments would give rise to positive gravity anomalies rather than negative. This observation rather contradicts the interpretation of low-gravity anomalies of the region with the thick light sediments.

c. The Mid-Mediterranean Ridge, known to be a highly distorted thick cover of sediments, having given no gravity anomaly is another evidence against the interpretation of the gravity anomalies of the region with sediments.

d. Woodside and Bowin (1970), comparing free-air and Bouguer anomalies in the region, determined that the cause of the anomalies should lie in the variation of the thickness of the crust. Therefore the interpretation of gravity anomalies based on sediment thickness variations is also in contradiction with the nature of the anomalies in the region.

e. Strange gravity-elevation relations in the region cannot be explained by sediments. These relations being inverse, indicate that the cause of the anomalies should lie within the mantle.

f. In the Eastern Mediterranean Basin, actual thicknesses of sediments have not been determined. Anhydrites of Miocene age recovered from the sea bottom indicate that the Eastern Mediterranean Basin might be younger than it is thought. Therefore the sediments in this basin might be much thinner than it is often assumed.

g. The interpretation of gravity anomalies based on sediments or the crustal thickness variations cannot explain the strange isostatic relations that prevail in the region. These relations require that the cause of the anomalies should lie within the mantle.

2. Interpretation of gravity anomalies based on the thickness variation of the crust cannot be reconciled with the following facts:

a. The Eastern Mediterranean Basin's 100-milligal low-gravity anomaly continues over Anatolia as 100-milligal excess anomaly. Normal crustal thickness variations should, in fact, produce a reverse effect as normally crust should be thicker over continents and thinner over oceans. In the region, the above-mentioned inverse relation cannot be explained by the variation of crustal thickness.

b. The rising of undercompensated regions and the sinking of overcompensated regions cannot be reconciled with normal crustal thickness variations.

The two above observations require that the cause of the gravity anomalies should lie within the mantle. Recent developments indicate that a phase change in the mantle and the formation of a low-velocity asthenosphere can explain the strange characteristics and relations of the gravity anomalies in the region. With the interpretation of individual anomalies with strange characteristics and relations, the above statement can further be elucidated.

3. Interpretation of some of the individual anomalies may be summarized as follows:

a. The Cyprus anomaly, one of the most interesting anomalies of the region, has been studied by many authors. Harrison (1955) observed the complex nature of the Cyprus anomaly consisting of a broad deep-seated anomaly and a high gradient near-surface anomaly superimposed on it. He suggested that the high gradient near-surface anomaly was caused by the Troodos Massif.

In Figure 1 the near-surface high gradient anomaly of the Troodos Massif is well defined by the 160-milligal and the deep-seated broad anomaly by the 100-milligal contour lines. The broad anomaly at its western side has been disturbed by the extension of the Troodos Massif towards north, evidenced by the nosing of contour lines in this zone.

The Cyprus anomaly while terminating suddenly at its western end, northern sides continue with linear gradient over into Anatolia until it is disturbed by the Taurus Range gravity minimum in the north. This suggests that Cyprus lies in the same general gravitational zone as Anatolia, with a general 100-milligal excess gravitational anomaly when compared with isostatically compensated zones.

The positive isostatic anomaly or isostatically undercompensated nature of Cyprus in the Eastern Mediterranean Basin which is in general overcompensated is thus explained.

The high positive Bouguer anomaly in Cyprus can then be explained by its undercompensated nature and the local near-surface anomaly caused by the heavy mass of the Troodos Massif superimposed on this high-gravity value.

The rising of Anatolia is evidenced by widespread rejuvenated river beds all over Anatolia. The rising of Cyprus has been proved by Harrison (1955) through observations of rejuvenated river beds and elevated coastal lines.

To explain the rising of these undercompensated zones, it is imperative to accept the presence of a rising force below the crust or within the mantle.

A phase change in the mantle, through decrease of density and increase of volume will provide for the necessary rising force within the mantle to raise overcompensated zones. Under the tectonic stresses in the region, asthenosphere formed by phase changes will raise these areas to a point where undercompensation will prevail, such as it is with Anatolia and Cyprus, and still continue raising these areas under regional tectonic stresses and phase changes.

The phase changes in the mantle will provide large amounts of volcanic and mantle material to be added to the crust to provide for the heavy masses to cause large near-surface gravity anomalies.

Therefore, the presence of an asthenosphere under regional tectonic stresses in the region, explains the undercompensated character of Anatolia and Cyprus; and their rising with the mantle under such conditions explains the inverse relation of gravity and elevation. It also explains the near-surface high-gravity anomalies caused by heavy masses, such as the Troodos Massif.

It is observed with interest that the Cyprus zone is distinctively different from other overcompensated zones of the Eastern Mediterranean Basin in that it is characterized by active volcanism. This is true for Anatolia and Aegean Sea too, which is important evidence for the presence of an asthenosphere under tectonic stresses in this region.

The local Silifke-Gulf of Mersin and the Adana Plain-Gulf of İskenderun anomaly couples with their inverse relation to normal isostatic conditions indicate local blocks, rising or sinking over the asthenosphere.

From these anomaly couples it is apparent that rising blocks over the asthenosphere give positive gravity anomalies or gravity highs and sinking blocks give negative gravity or gravity lows, an inverse relation between gravity and elevation. Normally the presence of an asthenosphere, due to density decrease, will cause a general overcompensation in the region. However in the Eastern Mediterranean Region, undercompensation conditions are not uncommon. These conditions may be explained by tectonic stresses. However sinking block movements—as indicated by local anomaly

couples in the Silifke- Gulf of Mersin and the Adana Plain- Gulf of İskenderun region and their associated gravity minimums together with inverse gravity elevation relations—cannot be explained simply by the presence of asthenosphere.

The answer to this question lies in the formation of grabens and rift systems. The crust lifted by asthenosphere will be under conditions of tension which will provide for the formation of grabens or rifts. Formation of rifts or grabens in the crust, as is well known, causes the crust to sink into the mantle under normal gravitational attraction until isostatic compensation condition is reached. Therefore the presence of asthenosphere also explains downward movement of the crust and the inverse gravity-elevation relations in these zones. The gravity minimum or undercompensation of such zones can also be explained by the presence of asthenosphere with its general low density.

b. Anomaly no. 3 in Figure 1, covering a large portion of the Eastern Mediterranean Basin, is characterized by being undercompensated with 100-milligal lower-gravity value than other similar regions that are compensated. Considering this zone as a sinking block over the asthenosphere conforms with the bathymetric data too. The zone being quiet both with respect to its magnetic anomalies and volcanic activity also supports the above consideration.

This zone is bordered to the north by the Mid-Mediterranean Ridge which is known to consist of highly deformed thick sediments. As no noticeable gravity anomaly could be associated with this zone, it cannot be considered as a deep-seated or major structural unit in the region. Seismic data indicate that this structural unit is formed by thrust sediments from north to south (Rabinowitz and Ryan, 1970), with formations dipping towards north.

Ocean bottom samples taken from this zone by the Woods Hole Oceanographic Institution, indicate that part of the Mid-Mediterranean Ridge was a part of the Nile Delta until Pliocene times. In the same investigation, evidence for compressional tectonics was also observed in this zone. This observation requires that Anomaly no. 3 Zone should be a young geological depression zone, sunk after Pliocene time to separate the Mid-Mediterranean Ridge from the Nile Delta, which is a good evidence to interpret gravity Anomaly no. 3 as a zone of sinking block over the asthenosphere.

The Mid-Mediterranean Ridge being a minor and near-surface structure, appears to be a highly deformed heap of overthrust sediments carried down from the north by gravity slides.

The arc-shaped gravity maximum to the south of Crete, including Anomalies no. 6, 11, 13 and 14, separated by gravity minimums defined by zero contours, has been considered by Rabinowitz and Ryan as the trench zone of the Cretan Island Arc. In large-spaced gravity profiles continuous arc-like gravity minimum was determined in this zone which was later, with the addition of further gravity data, broken up into alternating gravity highs and lows as shown in Figure 1.

In this zone some of the important abyssal plains of the Eastern Mediterranean Basin, such as the Pliny Trench, the Strabo Trench, the Rhodes Abyssal Plain and the Antalya Abyssal Plain occur. In Figure 1 it is observed that these zones have not given any significant gravity anomalies. This indicates that they are only minor local geological structures in the region. The gravity anomalies in the zone, with no relation to the surface expression of the geological structures must have their origin at depth. It is suggested that the gravity anomalies mark the crustal blocks which have risen or sunk over the asthenosphere, risen blocks giving the gravity maximums and sunken alternating blocks giving the gravity minimums. Harrison (1955) has observed the inverse gravity-elevation relation in this zone and has explained this observation with the rising and sinking of the crustal blocks together with the mantle.

The zone is in general overcompensated, indicating a sunken zone over the asthenosphere.

d. Straight to the south of Crete a zone of local gravity closures occurs, the bathymetric map in Figure 3 indicates that this zone is a shallow zone. The characteristics of near-surface anomalies of the region are seen in the anomalies of this zone. A comparison of the anomalies of this zone with the other anomalies of the region clearly indicates the necessity of relating other anomalies to deeper zones.

e. The gravity minimum extending from Crete to Rhodes and from there over Anatolia to Ankara is one of the conspicuous anomalies of the region. This zone forms an arc-like tectonic rise or a range in the alternative series of basin and range-type tectonic evolution of the region. This zone separates the two basins, one in the north marked by gravity Anomaly no. 17 which is considered by many authors to be the back deep of the Cretan Arc and the other one in the south marked by the arc-like gravity maximum running to the south of Crete.

This zone being in general undercompensated, is a zone where the crust has been raised by the mantle, over the asthenosphere.

f. Anomaly no. 17 is another one of the conspicuous anomalies of the region. This region, with its positive 150-milligal isostatic anomaly is undercompensated. In general the zone forms a basin in the region indicating a general crustal sinking. Normally crustal sinking over asthenosphere should produce a gravity low whereas in this zone a gravity high has been recorded. In this respect this anomaly zone may be compared with the Cyprus zone. Being in the general zone of undercompensation of Anatolia, the zone's undercompensated condition can be explained. However the gravity maximum associated with this zone in the general undercompensated zone of Anatolia and the Aegean region requires the assumption of the presence of heavier mass in this zone. This zone therefore may well compare with the Troodos Massif Zone in Cyprus. The inverse gravity elevation relations observed in this zone suggest that the cause of the anomaly lies within the mantle. The mantle in this zone has risen closely conforming with the topographic elevation to produce 100-milligal excess gravity value and to give rise to undercompensated conditions. Under conditions of tension the crust in this zone has also sunk to a certain extent to produce the present basin. The heavy near-surface materials on the other hand produce gravity high to produce the observed gravity anomaly in this zone. Part of the Bouguer gravity value in this zone is also due to its being in the water-covered area where normally one expects to find positive Bouguer gravity anomalies.

g. When local anomalies are not considered, the Eastern Mediterranean Region may be divided into two contrasting major gravity zones. These two zones are:

1. The zone to the north of the northern boundary of the arc-like gravity maximum running to the south of Crete.

2. The zone to the south of the same boundary.

The southern zone is bordered by a line running along the western limit of the Cyprus anomaly in the east and over Anatolia in the north, it is bordered by the Lake District Region.

The northern zone, on the other hand, includes the whole of Anatolia, the Aegean Sea and Cyprus, covered by the present gravity survey.

The northern and southern zones are characterized by being undercompensated and overcompensated respectively.

The two zones showing a typical inverse relation between gravity values and elevation requires that the cause of their gravity anomalies should lie within the mantle. The gravity anomaly characteristics of the two zones indicate that the northern zone is an elevated and the southern zone is a sunken zone over the asthenosphere.

The two zones in their general isostatic conditions include local gravity anomalies. As the local anomalies also show inverse relation between gravity values and elevation, this requires that the cause of these local anomalies should also lie within the mantle or within the vertical movements of the local crustal blocks over the asthenosphere. The Taurus Basin gravity anomaly, the south of Crete gravity maximum, the south of Cyprus gravity minimum, the Crete-Rhodes-Ankara gravity minimum and anomaly couples of Adana-İskenderun and Silifke-Mersin provide excellent examples for local anomalies produced by vertical movements of local blocks over the asthenosphere.

In addition to vertical block movements, heavy mantle material also gives rise to gravity anomalies in the region. Excellent examples for such anomalies are provided by the Cyprus and Cretan Island Arc back deep anomaly—Anomaly no. 17.

In Anatolia, Afyon, Konya-Tuz Gölü, Kayseri and Erzurum gravity anomalies also provide excellent examples for local gravity anomalies caused by local vertical crustal movements.

The Nile Delta gravity anomaly has been explained by others to be caused by the excess mass of sediments of the Nile Delta which is supported by the crust. It is not possible to prove the opposite of this explanation nor are we inclined to prove it, as the explanation given by others is considered as sound an explanation as there could be.

CONCLUSIONS

The conclusions reached through the study of the gravity anomalies of the Eastern Mediterranean region may be summarized as follows:

1. Interpretations of gravity anomalies in the Eastern Mediterranean Region based on the sedimentary thickness variations and on the thickness variations of the crust fall short in explaining the strange inverse relation between gravity anomalies and elevation, the strange isostatic conditions in the region and the crustal block movements defying normal isostatic conditions.

2. The following were derived from the analysis of gravity value and elevation relations:

- a. Anatolia, with its 2000-meter elevation, gives 100-milligal excess gravity Bouguer anomaly value; whereas Eastern Mediterranean Basin with its negative elevation gives 100-milligal low-gravity Bouguer anomaly value. This provides an excellent example for the inverse relation between gravity values and elevation.

- b. The inverse relation between gravity values and elevation is also true for local gravity anomalies in the region. Comparison of gravity values with topographic elevation readily indicates that the gravity anomalies of Adana Plain, Gulf of İskenderun, Silifke, Gulf of Mersin provide excellent examples for such local anomalies.

- c. A comparison of the bathymetric map and the gravity anomalies of the Eastern Mediterranean Basin readily indicates that the same inverse relation is true for the local anomalies included in the gravity maximum to the south of Crete and the Anomaly no. 17.

- d. The Cyprus anomaly provides an excellent example of inverse relation with its positive high-gravity value.

e. The same inverse relations were determined in the analysis of linear correlation coefficients between the gravity values and elevation along the profiles taken in the Taurus and Orhaneli regions.

f. It has been determined that the terrain correction constant calculated from regression coefficients was considerably different than the one normally used in gravity calculations.

g. Average Bouguer anomaly values calculated from the intercept of the regression lines were shown to have inverse relation with average elevation.

3. The inverse relation between gravity values and elevation determined in the region was interpreted as sufficient evidence to imply that the anomalies of the region were caused by vertical movements of crustal blocks together with the mantle, as was suggested by Harrison (1955) previously.

4. The gravity anomalies of the region require that the mantle should be at a higher elevation under Anatolia than under the Eastern Mediterranean Basin. This could be possible in either of the two cases below:

1) The crustal thickness in the Eastern Mediterranean Basin is larger than in Anatolia.

2) The crustal thickness is constant all over the region but the mantle is at a higher elevation under Anatolia than the Eastern Mediterranean Basin through uparching of the crust in Anatolian region.

As no information about the crustal thickness in the region is available, choosing one of the two cases from gravity data alone is rather impossible. However, abnormal isostatic block movements and inverse gravity value-elevation relations indicate that the second case is the more likely situation in the region.

5. In the region, the crustal blocks, which should sink under normal isostatic conditions are rising and the crustal blocks, which should rise under normal isostatic conditions are sinking. These abnormal isostatic crustal block movements are evidenced by several examples in the region.

Anatolia with its 100-milligal excess gravity anomaly value is rising although normally it should sink. The Eastern Mediterranean Basin with its 100-milligal low-gravity anomaly value should normally rise, but with its deep basins it is readily evidenced that it is a sunken basin including very young basins most probably still sinking.

Cyprus with its high-positive gravity anomaly value should normally be sinking, but it is evidenced that it is actually rising.

6. The above abnormal isostatic crustal movements require the acceptance of the presence of a lifting force in the mantle which causes the upward and downward movement of the crust defying normal isostatic conditions.

7. Recent developments indicate that the lifting force in the mantle can be produced by phase changes in the mantle.

In the light of the recent developments and the inverse relation between gravity values and elevation, and abnormal isostatic block movements, it is suggested that in the region there exists an asthenosphere formed by the phase changes in the mantle.

8. Phase changes in the mantle cause an increase in volume, hence causing a lifting force in the mantle. This lifting force readily explains the upward movements of the crustal blocks. However it cannot explain the downward movement of the crustal blocks.

9. The downward movement of the crustal blocks requires the uparching of the crust with the mantle.

Uparching of the crust produces tension conditions in the crust, which in turn produce graben formations. Formation of grabens explains the downward crustal movements in the region.

10. The 100-milligal low-gravity anomaly value of the Eastern Mediterranean Basin is explained by the low density of the asthenosphere and the 100-milligal excess gravity anomaly value of Anatolia is explained by the uparching of Anatolian crust above the asthenosphere together with the mantle, thus bringing mantle material to higher levels. This condition requires the acceptance of the presence of tectonic stress conditions in the region.

11. The local gravity anomalies of the region are related to local crustal block movements to form local grabens and horsts in the general gravitational conditions of the region.

12. The lifting force of the asthenosphere readily explains the abnormal upward crustal movements. Rising and sinking of the asthenosphere with the crustal blocks explain the inverse gravity value-elevation relations and uparching of the crust with the lifting force of the asthenosphere explains the abnormal downward crustal movements in the region. As the presence of an asthenosphere explains all the abnormal characteristics of the gravity anomalies in the region, it forms the most important evidence for the connection of the cause of the anomalies to the phase change in the mantle.

13. The results of this investigation indicate that the gravitational studies in connection with the tectonic evolution of the region would be an interesting area for further study.

ACKNOWLEDGEMENTS

I wish to thank Professor İhsan Özdoğan for his kind acceptance to supervise this doctorate thesis submitted to the Faculty of Science, Institute of Geophysics of the University of İstanbul and for the assistance with his enlightening advice and criticism on the preparation of the thesis; Professor Mehmet Dizioğlu for his constant encouragement and advice in starting this study; Doc. Dr. Sadrettin Alpan, General Director of the Mineral Research and Exploration Institute, for his unending assistance in all phases of the preparation and performance of this thesis and for making possible the delivery of part of the thesis at the annual convention of E.A.E.G at Hannover; Dr. Turan Kayıran for assisting in the computer analysis of the gravity data; Professor Melih Tokay, Professor Brinkmann, Dr. Teoman Norman, Dr. Sırrı Kavlakoğlu for their generous assistance in the final preparation of the thesis through reading and criticising the text and advising; Professor Kazım Ergin and Professor İhsan Ketin for their encouragement with their criticisms; Ratıp Özakçay, Ferit Erden, Recai Şener, Güner Özelçi, Baki İnsel, Bekir Özgirgin, Necmiye Tulgar and others for their generous assistance in the typing, drafting and formatting of this thesis.

MULTIPLE CORRELATION

Coefficient.

SUBROUTINE MULTR (N,K, XBAR, STD, D, RX, RY, ISAVE, B, SB, T, ANS) DIMENSION XBAR
(1), STD (1), D (1), RX (1), RY (1), ISAVE (1), B (1), SB (1), T (1), ANS (10)
MM=K+1

```
C          BETA WEIGHTS
DO 100 J=1,K
100  B(J)=0.0
      DO 110 J=1,K
      L1=K (J-1)
      DO 110 I=1,K
      L=L1+1
110  B(J)=B (J)+RY (I) RX (L)
      RM=0.0
      BO=0.0
      L1=ISAVE (MM)
C          COEFFICIENT OF DETERMINATION
DO 120 I=1,K
RM=RM+B(I) RY (I)
C          REGRESSION COEFFICIENTS
L=ISAVE (I)
B (I) =B(I) (STD (L1)/STD(L))
C          INTERCEPT
120  BO=BO+B(I) XBAR (L)
      BO=XBAR (L)-BO
C          SUM OF SQUARES ATTRIBUTABLE TO REGRESSION
SSAR=RM D(L1)
C          MULTIPLE CORRELATION COEFFICIENT
122  RM=SQRT (ABS(RM))
C          SUM OF SQUARES OF DEVIATIONS FROM REGRESSION
SSDR=D (L1)-SSAR
C          VARIANCE OF ESTIMATE
FN=N-K-1
SY=SSDR/FN
C          STANDARD DEVIATIONS OF REGRESSION COEFFICIENTS
DO 130 J=1,K
L1=K (J-1)+J
L=ISAVE (J)
125  SB (J) = SQRT (ABS ((RX(L1)/D(L)) SY))
C          COMPUTED T-VALUES
130  T Q)=B(J)/SB(J)
C          STANDARD ERROR OF ESTIMATE
135  SY=SQRTC ABS (SY))
C          F VALUE
FK=K
SSARM=SSAR/FK
SSDRM=SSDR/FN
F=SSARM/SSDRM
```

```
ANS (1) = BO
ANS (2) = RM
ANS (3) = SY
ANS (4) = SSAR
ANS (5) = FK
ANS (6) = SSARM
DEVIATIONS FROM REGRESSION LINE
DIMENSION X (2,100)
READ (2,101) CEPT
101  FORMAT (F9.4)
    READ (2,202) N
202  FORMAT (I2)
    READ (2,102) ((X(I,J), I 1,2), J 1,N)
102  FORMAT (2F7.2)
    WRITE (3,105) ((X(I,J), I 1,2), J 1,N)
105  FORMAT (2 F 10.2)
    DO 2 J 1,N
      B X (2J)-R X (1,J)-CEPT
    WRITE (3,201) B
201  FORMAT (/F10.3)
2    CONTINUE
    CALL EXIT
    END
ANS (7 ) = SDR
ANS (8) = FN
ANS (9 ) = SSARM
ANS (10) = F
RETURN
END
```

TAURUS PROFILE

Multiple regression STN: 1-33
 Selection1 Variable: x Dependent: y

<i>x</i>	<i>y</i>	<i>y</i> ₁	<i>y</i> ₂	<i>x</i>	<i>y</i>	<i>y</i> ₁	<i>y</i> ₂
1025.19	-278.05	38.32	-76.08	208.87	-136.02	-71.56	-85.47
1045.06	-277.63	44.88	-71.96	185.05	-132.75	-75.64	-89.09
1118.41	-292.30	52.84	-72.20	241.18	-146.01	-71.58	-93.81
1173.60	-304.01	58.16	-73.05	309.19	-161.47	-66.05	-97.77
1240.48	-321.21	61.60	-77.09	294.98	-160.97	-69.94	-101.35
1432.33	-359.86	82.16	-77.35	234.72	-148.48	-76.05	-101.87
1490.47	-370.55	89.41	-75.94	166.69	-134.41	-82.97	-100.87
1457.13	-366.31	83.36	-77.83	109.74	-126.11	-92.24	-103.51
1649.84	-406.96	102.18	-80.39	105.32	-123.16	-92.66	-103.60
1419.77	-363.64	74.50	-77.50	111.17	-123.98	-89.67	-101.69
1414.03	-362.40	73.97	-77.08	100.02	-120.57	-89.70	-99.97
1383.75	-358.94	68.09	-79.14	110.98	-119.55	-85.30	-96.79
1209.56	-329.77	43.50	-81.44	260.43	-147.39	-67.07	-95.33
932.25	-273.32	14.37	-79.85	300.34	-152.64	-59.96	-91.60
739.87	-235.65	-7.33	-89.95	228.65	-134.48	-63.92	-87.62
516.04	-193.33	-34.08	-85.04	187.10	-121.24	-63.50	-80.79
292.18	-151.51	-65.34	-83.89				

<i>Variable</i>	<i>Mean</i>	<i>Standard deviation</i>	<i>Correlation x VS y</i>	<i>Regression coefficient</i>	<i>Intercept</i>
Elevation <i>x</i>	-637.707	550.202			
Dependent					
Observed <i>y</i>	-225.353	100.154	-0.998	-0.181	-100.878
Free-air <i>y</i> ₁	-13.126	70.085	0.996	0.126	-99.777
Bouguer <i>y</i> ₂	-86.875	10.459	0.815	0.015	-97.192

Deviation from regression line

<i>Sy-A</i>	<i>Sy₁-O</i>	<i>Sy₂-x</i>	<i>Sy-A</i>	<i>Sy₁-O</i>	<i>Sy₂-x</i>
9.091	8.003	5.214	2.807	1.712	8.483
13.121	12.042	9.025	1.749	0.645	5.233
11.778	10.694	7.648	-1.313	-2.408	-0.358
10.095	9.011	5.942	-4.416	-5.508	-5.373
5.046	3.964	0.865	-6.498	-7.595	-8.732
1.253	0.178	-2.371	-4.956	-6.058	-8.318
1.126	0.051	-1.862	-3.246	-4.345	-6.263
-0.632	-1.769	-3.235	-5.293	-6.388	-8.019
-6.329	-7.403	-8.784	-5.146	-6.247	-8.041
-4.809	-5.888	-2.326	-2.903	-4.000	-6.222
-4.612	-5.689	-1.817	-1.519	-2.615	-4.329
-6.654	-7.727	-3.407	1.492	0.394	-1.319
-9.132	-10.213	-3.006	0.805	-0.290	-2.176
-3.065	-4.153	2.885	2.806	1.705	0.935
-0.348	-1.400	-4.232	7.941	6.842	6.027
1.286	0.213	4.150	3.632	12.535	13.501
2.453	1.361	8.771			

<i>Difference of intercept</i>	<i>Difference of reg. coef. (-)</i>	<i>Ratio of reg. coef.</i>
A - O = -1.101	<i>y</i> - <i>y</i> ₁ = 0.307	<i>y</i> / <i>y</i> ₁ = -1.436
A - <i>x</i> = -3.686	<i>y</i> - <i>y</i> ₂ = 0.196	<i>y</i> / <i>y</i> ₂ = -12.066
O - <i>x</i> = -2.585	<i>y</i> ₁ - <i>y</i> ₂ = -0.111	<i>y</i> ₁ / <i>y</i> ₂ = 8.400

TAURUS PROFILE

Multiple regression STN: 34-46
 Selection 1 Variable: x dependent: y

<i>x</i>	<i>y</i>	<i>y</i> ₁	<i>y</i> ₂	<i>x</i>	<i>y</i>	<i>y</i> ₁	<i>y</i> ₂
248.73	- 118.59	- 41.83	- 64.11	217.17	- 86.36	- 19.34	- 42.88
274.91	- 119.81	- 34.97	- 60.41	134.58	- 69.78	- 28.25	- 42.44
161.44	- 93.42	- 43.60	- 54.85	71.59	- 56.39	- 34.30	- 40.82
43.63	- 63.71	- 50.25	- 48.15	13.54	- 43.58	- 39.40	- 40.52
35.64	- 60.52	- 49.52	- 46.76	7.97	- 40.39	- 37.93	- 36.28
60.95	- 63.32	- 44.51	- 44.17	5.27	- 36.15	- 34.52	- 33.43
137.12	- 73.02	- 30.70	- 42.74				

<i>Variable</i>	<i>Mean</i>	<i>Standard deviation</i>	<i>Correlation x VS y</i>	<i>Regression coefficient</i>	<i>Intercept</i>
Elevation x	108.656	94.157			
Dependent					
Observed y	- 71.156	26.971	- 0.954	- 0.273	- 41.50
Free-air y ₁	- 37.624	8.673	0.381	0.035	- 41.42
Bouguer y ₂	- 45.966	8.966	- 0.765	- 0.072	- 38.15

Deviation from regression line

<i>Sy-A</i>	<i>Sy₁-O</i>	<i>Sy₂-x</i>	<i>Sy-A</i>	<i>Sy₁-O</i>	<i>Sy₂-x</i>
- 9.67	- 9.139	- 7.820	14.532	14.458	11.108
- 3.127	- 3.198	- 2.211	8.525	8.447	5.525
- 7.769	- 7.846	- 4.926	4.689	4.608	2.551
- 10.278	- 10.361	- 6.818	1.623	1.545	1.382
- 9.273	- 9.350	- 6.010	3.290	3.211	2.452
- 5.151	- 5.229	- 1.575	6.792	6.716	5.105
5.981	5.908	5.410			

<i>Difference of intercept</i>	<i>Difference of reg. coef.</i>	<i>Ratio of reg. coef.</i>
A - O = - 0.080	y - y ₁ = 0.308	y/y ₁ = - 7.80
A - x = - 3.350	y - y ₂ = 0.201	y/y ₂ = 3.79
O - x = - 3.270	y ₁ - y ₂ = - 0.107	y ₁ /y ₂ = - 0.486

Multiple regression STN: 47-76
 Selection 1 Variable: x dependent: y

<i>x</i>	<i>y</i>	<i>y</i> ₁	<i>y</i> ₂	<i>x</i>	<i>y</i>	<i>y</i> ₁	<i>y</i> ₂
2.18	- 38.36	- 37.69	- 37.54	5.00	- 97.43	- 95.89	- 96.29
2.43	- 40.07	- 39.32	- 38.91	12.54	- 98.33	- 94.46	- 95.71
13.89	- 49.39	- 45.10	- 45.18	5.02	- 98.55	- 97.00	- 97.40
8.67	- 49.11	- 46.43	- 46.67	5.81	- 102.29	- 100.50	- 101.00
15.82	- 51.13	- 46.25	- 47.39	23.88	- 104.20	- 96.83	- 99.35
9.08	- 49.51	- 46.71	- 47.31	17.20	- 90.03	- 84.72	- 86.57
1.92	- 48.29	- 47.70	- 47.03	13.34	- 89.20	- 85.08	- 86.51
9.65	- 52.16	- 49.18	- 49.85	13.62	- 87.41	- 83.21	- 84.73
6.02	- 60.16	- 58.30	- 58.56	18.18	- 87.64	- 82.03	- 84.06
2.96	- 61.82	- 60.91	- 61.03	15.15	- 90.38	- 85.70	- 87.39
5.72	- 65.64	- 63.87	- 64.36	25.69	- 92.08	- 84.15	- 87.02
7.42	- 72.19	- 69.90	- 70.51	45.17	- 94.39	- 80.45	- 85.43
8.28	- 77.50	- 74.94	- 75.71				
14.14	- 86.48	- 82.12	- 83.54				
24.34	- 91.56	- 84.05	- 86.61				
14.40	- 92.12	- 87.68	- 89.10				
7.22	- 99.81	- 97.58	- 98.21				

<i>Variable</i>	<i>Mean</i>	<i>Standard deviation</i>	<i>Correlation x VS y</i>	<i>Regression coefficient</i>	<i>Intercept</i>
Elevation x	12 232	9.167			
Dependent					
Observed y	— 76.456	21.495	— 0.442	— 1.036	— 63.79
Free-air y ₁	— 72.680	20.402	— 0.327	— 0.728	— 63.78
Bouguer y ₂	— 73.757	20.996	— 0.371	— 0.850	— 63.36

Deviation from regression line

<i>Sy-A</i>	<i>Sy₁-O</i>	<i>Sy₂-x</i>	<i>Sy-A</i>	<i>Sy₁-O</i>	<i>Sy₂-x</i>
27.69	27.678	27.674	— 13.399	— 13.414	— 13.497
26.24	26.230	26.516	— 28.534	— 28.542	— 28.711
28.80	28.795	29.989	— 28.455	— 28.469	— 28.679
23.67	23.664	24.061	— 21.538	— 21.548	— 21.688
29.06	29.050	29.420	— 29.555	— 29.564	— 29.772
23.70	23.682	23.770	— 32.476	— 32.489	— 32.700
17.49	17.479	17.963	— 15.650	— 15.660	— 15.668
21.63	21.628	21.715	— 8.406	— 8.415	— 8.587
9.87	9.864	9.918	— 11.578	— 11.585	— 11.808
5.04	5.026	4.847	— 9.498	— 9.512	— 9.790
4.08	4.076	3.863	— 5.000	— 5.011	— 5.244
— 7.06	— 0.716	— 0.841	— 10.882	— 10.887	— 11.150
— 5.125	— 5.130	— 5.310	— 1.654	— 1.662	— 1.819
— 8.029	— 8.043	— 8.158	16.230	16.223	16.332
— 7.533	— 2.545	— 2.557			

Difference of intercept

A — O = — 0.01
A — x = — 0.43
O — x = — 0.42

Difference of reg. coef. (-)

y ₁ — y ₂ = — 0.122
y — y ₁ = 0.308
y — y ₂ = 0.186

Ratio of reg. coef.

y/y ₁ = 1.420
y/y ₂ = 1.220
y ₁ /y ₂ = 0.856

Multiple regression STN: 77-89

Selection 1 Variable: x dependent: y

<i>x</i>	<i>y</i>	<i>y₁</i>	<i>y₂</i>	<i>x</i>	<i>y</i>	<i>y₁</i>	<i>y₂</i>
114.79	— 93.87	— 58.45	— 70.37	623.56	— 228.89	— 36.46	— 101.93
187.96	— 107.56	— 49.56	— 69.28	753.95	— 255.91	— 23.24	— 103.44
278.22	— 129.01	— 43.15	— 71.95	876.10	— 285.94	— 15.58	— 106.64
260.98	— 131.28	— 50.74	— 78.95	1022.42	— 323.51	— 7.99	— 108.04
352.55	— 159.21	— 50.41	— 87.44	1195.34	— 356.36	— 12.52	— 114.18
536.20	— 201.64	— 36.17	— 92.67	1271.38	— 368.01	— 24.34	— 113.10
621.74	— 224.97	— 33.10	— 99.87				

<i>Variable</i>	<i>Mean</i>	<i>Standard deviation</i>	<i>Correlation x VS y</i>	<i>Regression coefficient</i>	<i>Intercept</i>
Elevation x	622.706	383.716			
Dependent					
Observed y	— 220.473	93.847	— 0.993	— 0.244	— 68.53
Free-air y ₁	— 28.306	25.433	0.973	0.064	— 68.76
Bouguer y ₂	— 93.681	16.434	— 0.947	— 0.040	— 68.77

Deviation from regression line

<i>Sy-A</i>	<i>Sy₁-O</i>	<i>Sy₂-x</i>	<i>Sy-A</i>	<i>Sy₁-O</i>	<i>Sy₂-x</i>
2.670	2.307	3.057	— 8.211	— 8.519	— 7.863
6.832	6.477	7.116	— 3.416	— 3.709	— 4.083
7.406	7.065	8.107	— 3.642	— 3.928	— 2.328
0.923	0.587	0.408	— 5.510	— 5.776	— 2.208
— 4.658	— 4.989	— 4.367	3.833	3.581	3.083
— 2.277	— 2.594	— 2.147	10.737	10.496	7.248
— 4.735	— 5.042	— 5.877			

<u>Difference of intercept</u>			<u>Difference of reg. coef. (-)</u>			<u>Ratio of reg. coef.</u>		
A - O =	- 0.37		y - y ₁ =	0.308		y/y ₁ =	- 3.212	
A - x =	0.24		y - y ₂ =	0.204		y/y ₂ =	6.100	
O - x =	0.61		y ₁ - y ₂ =	- 0.104		y ₁ /y ₂ =	- 1.600	
Multiple regression	STN: 90-95							
Selection	1 Variable: x Dependent: y							

<u>x</u>	<u>y</u>	<u>y₁</u>	<u>y₂</u>	<u>x</u>	<u>y</u>	<u>y₁</u>	<u>y₂</u>
1073.23	- 327.73	3.47	- 110.52	771.06	- 250.76	- 13.71	- 92.74
881.70	- 280.02	- 7.93	- 100.70	805.39	- 256.40	- 7.86	- 91.63
815.06	- 262.10	- 10.57	- 95.16	836.46	- 264.77	- 6.64	- 82.10

<u>Variable</u>	<u>Mean</u>	<u>Standard deviation</u>	<u>Correlation x VS y</u>	<u>Regression coefficient</u>	<u>Intercept</u>
Elevation x	863.816	108.919			
Dependent					
Observed y	- 273.629	28.280	- 0.998	- 0.259	- 49.90
Free-air y ₁	- 7.206	5.811	0.951	0.050	- 50.40
Bouguer y ₂	- 95.474	9.538	- 0.789	- 0.069	- 35.87

Deviation from regression line

<u>S_{y-A}</u>	<u>S_{y₁-O}</u>	<u>S_{y₂-x}</u>	<u>S_{y-A}</u>	<u>S_{y₁-O}</u>	<u>S_{y₂-x}</u>
0.359	- 0.639	- 0.410	- 0.995	- 2.471	- 3.532
- 1.576	- 2.311	- 3.809	2.263	1.635	- 0.047
- 0.930	- 1.566	- 2.908	1.947	1.277	11.632

<u>Difference of intercept</u>			<u>Difference of reg. coef. (-)</u>			<u>Ratio of reg. coef.</u>		
A - O =	0.50		y - y ₁ =	0.309		y/y ₁ =	- 5.180	
A - x =	- 14.03		y - y ₂ =	0.190		y/y ₂ =	3.753	
O - x =	- 14.53		y ₁ - y ₂ =	- 0.119		y ₁ /y ₂ =	- 0.725	
Multiple regression	STN: 96-105							
Selection	1 Variable: x Dependent: y							

<u>x</u>	<u>y</u>	<u>y₁</u>	<u>y₂</u>	<u>x</u>	<u>y</u>	<u>y₁</u>	<u>y₂</u>
863.07	- 254.81	11.53	- 69.94	1202.93	- 318.23	52.99	- 78.73
909.27	- 262.52	18.11	- 70.85	1252.88	- 323.29	63.35	- 74.57
967.19	- 277.52	20.95	- 76.42	1319.76	- 345.62	61.66	- 83.68
1085.46	- 297.42	37.55	- 78.00	1376.34	- 360.40	64.34	- 88.20
1177.07	- 313.88	49.36	- 79.88	1424.46	- 369.79	69.80	- 88.11

<u>Variable</u>	<u>Mean</u>	<u>Standard deviation</u>	<u>Correlation x VS y</u>	<u>Regression coefficient</u>	<u>Intercept</u>
Elevation x	1157.843	196.283			
Dependent					
Observed y	- 312.347	39.583	- 0.995	- 0.200	- 80.78
Free-air y ₁	44.963	21.508	0.984	0.107	- 78.93
Bouguer y ₂	- 78.837	6.376	- 0.891	- 0.028	- 46.42

Deviation from regression line

<u>S_{y-A}</u>	<u>S_{y₁-O}</u>	<u>S_{y₂-x}</u>	<u>S_{y-A}</u>	<u>S_{y₁-O}</u>	<u>S_{y₂-x}</u>
- 0.780	- 2.627	1.472	4.022	2.177	2.524
0.784	- 1.030	1.900	8.989	7.149	8.130
- 2.589	- 4.437	- 1.993	0.084	- 1.754	0.957
1.252	- 0.593	- 0.148	- 3.338	- 5.177	- 1.925
3.181	1.336	0.625	- 3.069	- 4.907	- 0.442

<u>Difference of intercept</u>			<u>Difference of reg. coef. (-)</u>			<u>Ratio of reg. coef.</u>		
A - O =	- 1.85		y - y ₁ =	0.307		y/y ₁ =	- 1.869	
A - x =	- 34.36		y - y ₂ =	0.172		y/y ₂ =	7.142	
O - x =	- 32.51		y ₁ - y ₂ =	- 0.135		y ₁ /y ₂ =	- 3.821	

TAURUS PROFILE

Multiple regression STN: 1-46
 Selection 1 Variable: x dependent: y

<u>Variable</u>	<u>Mean</u>	<u>Standard deviation</u>	<u>Correlation x VS y</u>	<u>Regression coefficient</u>	<u>Intercept</u>
Elevation x	524.062	535.838			
Dependent					
Observed y	- 181.775	110.700	- 0.982	- 0.202	- 75.429
Free-air y ₁	- 20.049	60.311	0.938	0.105	- 75.428
Bouguer y ₂	- 75.314	21.120	- 0.154	- 0.006	- 72.132
<u>Difference of intercept</u>			<u>Difference of reg. coef. (-)</u>		<u>Ratio of reg. coef.</u>
A - O = 0			y - y ₁ = 0.307		y/y ₁ = 2
A - x = -3.30			y - y ₂ = 0.192		y/y ₂ = 20
O - x = -3.30			y ₁ - y ₂ = 0.111		y ₁ /y ₂ = 11

Multiple regression STN No: 47-75
 Selection 1 Variable: x dependent y

<u>Variable</u>	<u>Mean</u>	<u>Standard deviation</u>	<u>Correlation x VS y</u>	<u>Regression coefficient</u>	<u>Intercept</u>
Elevation x	11.056	6.748			
Dependent					
Observed y	- 75.815	21.605	- 0.464	- 1.486	- 59.378
Free-air y ₁	- 72.403	20.721	- 0.383	- 1.178	- 59.378
Bouguer y ₂	- 72.104	21.914	- 0.297	- 1.034	0.741
<u>Difference of intercept</u>			<u>Difference of reg. coef. (-)</u>		<u>Ratio of reg. coef.</u>
A - O = 0.000			y - y ₁ = 0.308		y/y ₁ = 1.3
A - x = 2.315			y - y ₂ = 0.452		y/y ₂ = 1.3
O - x = 2.315			y ₁ - y ₂ = 0.144		y ₁ /y ₂ = 1.1

Multiple regression STN No: 76-105
 Selection 1 Variable x vs y

<u>Variable</u>	<u>Mean</u>	<u>Standard deviation</u>	<u>Correlation x VS y</u>	<u>Regression coefficient</u>	<u>Intercept</u>
Elevation x	830.055	390.807			
Dependent					
Observed y	- 257.526	83.016	- 0.985	- 0.209	- 83.772
Free-air y ₁	- 1.401	41.295	0.939	0.099	- 83.760
Bouguer y ₂	- 88.415	12.923	- 0.266	- 0.007	- 83.086
<u>Difference of intercept</u>			<u>Difference of reg. coef. (-)</u>		<u>Ratio of reg. coef.</u>
A - O = - 0.012			y - y ₁ = 0.308		y/y ₁ = - 2.1
A - x = - 0.686			y - y ₂ = 0.202		y/y ₂ = 29.8
O - x = - 0.674			y ₁ - y ₂ = - 0.106		y ₁ /y ₂ = - 14.1

ORHANEĪI PROFILE

Multiple regression STN No: 1-27
 Selection 1 Elevation x vs y observed

<u>Variable</u>	<u>Mean</u>	<u>Standard deviation</u>	<u>Correlation x VS y</u>	<u>Regression coefficient</u>	<u>Intercept</u>
Elevation x	531.629	131.529			
Dependent					
Observed y	82.313	35.578	- 0.943	- 0.255	
Observed y ₁	83.644	35.177	- 0.941	- 0.251	

RESULTS OF GRAVITY ANALYSIS
TAURUS REGION

Stn. no.	Variable	Mean	Standard deviation	Correlation coefficient	Regression coefficient	Intercept	Regression coefficient		
							Intercept difference	Difference	Ratio
							A-O A-x O-x	y-y ₁ y-y ₂ y ₁ -y ₂	y/y ₁ y/y ₂ y ₁ /y ₂
1-33	x	687.707	550.20	—	—	—	—	—	—
	y	-225.353	100.154	-0.99815	-0.181	-100.878	-1.101	0.307	-1.438
	y ₁	-13.126	70.086	0.99623	0.126	-99.777	-2.585	0.196	-12.066
	y ₂	-86.876	10.459	0.81578	0.015	-97.192	-3.686	-0.111	8.400
34-46	x	108.657	94.158	—	—	—	—	—	—
	y	-71.157	26.972	-0.95478	-0.273	-41.50	-0.080	0.308	-7.80
	y ₁	-37.625	8.674	0.38105	0.035	-41.42	-3.350	0.201	3.79
	y ₂	-45.966	8.967	-0.76586	-0.072	-38.15	-3.270	-0.107	-0.486
47-76	x	12.232	9.168	—	—	—	—	—	—
	y	-76.456	21.495	-0.44220	-1.036	-63.79	-0.01	0.308	1.420
	y ₁	-72.681	20.403	-0.32720	-0.728	-63.78	-0.43	0.186	1.220
	y ₂	-73.758	20.997	-0.37123	-0.850	-63.36	-0.42	-0.122	0.856
77-89	x	622.707	383.717	—	—	—	—	—	—
	y	-220.474	93.847	-0.99805	-0.244	-68.53	-0.37	0.308	-3.812
	y ₁	-28.307	25.434	0.97313	0.064	-68.16	0.24	0.204	6.100
	y ₂	-93.681	16.434	-0.94718	-0.040	-68.77	0.61	-0.104	-1.600
90-95	x	863.817	108.919	—	—	—	—	—	—
	y	-273.630	28.281	-0.99834	-0.259	-49.90	0.50	0.309	-5.180
	y ₁	-7.207	5.811	0.95193	0.050	-50.40	-14.03	0.190	3.753
	y ₂	-95.475	9.538	-0.78998	-0.069	-35.87	-14.53	-0.119	-0.725
96-105	x	1157.843	196.283	—	—	—	—	—	—
	y	-312.348	39.583	-0.99538	-0.200	-80.78	-1.85	0.307	-1.869
	y ₁	44.964	21.508	0.98428	0.107	-78.93	-34.36	0.172	7.142
	y ₂	-78.838	6.376	-0.89145	-0.028	-46.42	-32.51	-0.135	-3.821
1-46	x	524.062	535.838	—	—	—	—	—	—
	y	181.775	110.700	-0.982	-0.202	-75.429	0.001	0.307	2
	y ₁	-20.049	60.311	0.938	0.105	-75.428	-3.30	0.152	20
	y ₂	-75.314	21.120	+0.154	-0.006	-72.132	-3.30	-0.111	—
47-75	x	11.056	6.748	—	—	—	—	—	—
	y	-75.815	21.605	-0.464	-1.486	-59.378	0.000	0.308	1.3
	y ₁	-72.403	20.721	-0.383	-1.178	-59.378	2.315	0.452	1.5
	y ₂	-72.104	21.914	-0.297	-1.034	-61.693	2.315	0.144	1.14
76-105	x	830.055	390.807	—	—	—	—	—	—
	y	-257.526	83.016	-0.985	-0.209	-83.772	-0.012	0.308	-2.1
	y ₁	-1.401	41.295	0.939	0.099	-83.760	-0.686	0.202	29.8
	y ₂	-88.415	12.923	-0.266	-0.007	-83.086	-0.674	-0.106	-14.1

ORHANELI PROFILE

1-27	x	531.629	131.529	—	—	—	—	—	—
	y	82.313	35.578	-0.943	-0.255	—	—	—	—
	y ₁	83.644	35.177	-0.941	-0.251	—	—	—	—

R E F E R E N C E S

- AKI, K. & PRESS, F. (1961): *Geophys. Jour.*, v. 5, p. 292.
- ALLAN, T.D. et al. (1964): *Nature*, n. 204, p. 1245.
- BELOUSSOV, V.V. (1964): *Tectonophysics*, 1969, v. 7, p. 588.
- BERRY, M.J. & KNOPFT, I. (1967): *J. Geophys. Res.*, v. 72, n. 14, p. 3613.
- BIRCH, F. (1960): *J. Geophys. Res.*, v. 65, p. 1083.
- (1961): *J. Geophys. Res.*, v. 66, p. 2199.
- BOLT, B.A. & NUTTLI, O.W. (1966): *J. Geophys. Res.*, v. 71, p. 5977.
- CARDER, D.S. et al. (1966): *Bull. Seis. Soc. Amer.*, v. 56, p. 815.
- CARTER, J.L. (1970): *Geol. Soc. Amer. Bull.*, v. 81, p. 2021.
- CHRISTENSEN, N.I. (1968): *Tectonophysics*, v. 6, p. 331.
- & CROSSON, R.S. (1968): *Tectonophysics*, v. 6, n. 2, p. 93.
- CLARK, Jr. S.P. & RINGWOOD, A.F. (1964): *Rev. Geophys.*, v. 2, p. 36.
- CLEARY, J.R. & HALES, A.L. (1966): *Bull. Seis. Soc. Amer.*, v. 56, p. 467.
- (1966): *Nature*, n. 210, p. 619.
- COOPER, R.I.B. et al. (1952): *Phil. Trans. Roy. Soc. London, ser. A*, 244, p. 533.
- EMERY et al. (1966): *Deep Sea Res.*, v. 13, p. 173.
- EWING, J. & EWING, M. (1959): *Geol. Soc. Amer. Bull.*, v. 70, p. 291.
- GASS, I.G. (1967): *Ultramafic and related rocks*, Editor: P.J. Wyllie, Pub. Willey, N.Y. p. 121.
- (1968): *Nature*, n. 220 p. 39.
- & MASSON, - SMITH, D. (1963): *Phil. Trans. Roy. Soc. London, ser. A*, 255, p. 417.
- GASKELL, T.F. and others (1958): *Phil. Trans. Roy. Soc. London, ser. A*, 251, p. 28.
- GREEN, D.H. & RINGWOOD, A.E. (1967): *Earth Planetary Ltrs*, v. 3, p. 151.
- GUTTENBERG, B. (1959): *Ann. Geofis.* v. 12, p. 439.
- HALES, A.L. et al. (1968): *Jour. Geophys. Rts.*, v. 73, p. 3885.
- HARRIS, P.G. et al. (1967): *Jour. Geophys. Res.*, v. 72, p. 6359.
- HARRISON, J.C. (1955): *Phil. Trans. Roy. Soc. London, ser. A*, 248, p. 283.
- HERRIN, E. (1966): *Trans. Amer. Geophys. Union (Abstract)*, v. 47, p. 44.
- IBM Application program, H 20-0205-3, System/360 Scientific Subroutine Package (360 A-CM-03 X) Version III, Programmer's manual.
- IBRAHIM, A.K. & NUTTLI, O.W. (1967): *Bull. Seis. Soc. Amer.*, v. 57, p. 1060.
- KING HELE, D.d. (1962): *Geophys. Jour.*, v. 6, p. 270.
- MELLIS, O. (1954): *Dead Sea Res.*, v. 2, n. 2 p. 89.
- MORONEY, M.J. (1958): *Facts From Figures*, Penguin Books Ltd., Harmondsworth, Middlesex, England.
- NUTTLI, O. (1963): *Rev. Geophys.*, v. 1, p. 351.

- OLAUSSON, E. (1961): Swedish Deep Sea Exped. Rep., v. 8, n. 4, p. 335.
- OXBURGH, E.R. (1964): Geophys. Jour., v. 8, p. 456.
- RABINOWITZ, P.D. & RYAN W.B.F. (1970): Tectonophysics, v. 10, p. 585,
- RITSEMA, A.R. (1970): Tectonophysics, v. 10, p. 609.
- RYAN, W.B.F. et al. (1965): Geol. Soc. Amer. Bull., v. 76, p. 1261.
- ; STANLEY, D.J.; HERSEY, J.B.; FAHLQUIST, D.A. & ALLAN, T.D. (1970): The Sea, Editor: A. Maxwell Pub. Willey, N.Y., p. 387.
- TOKSÖZ, N.M. & HAMED, J.A. (1968): Trans Amer. Geophys. Union, v. 49, p. 289.
- WOLLARD, (1962): Jour. of Geophys. Research.
- WONG, H.K. & ZARUDZKI, E.F.K. (1969): Geol. Soc. Amer. Bull, v. 80, p. 2611.
- WOODSIDE, J. & BOWIN, C. (1970): Geol. Soc. Amer. Bull., v. 81, p. 1107.